Supplement of Solid Earth, 11, 37–62, 2020
https://doi.org/10.5194/se-11-37-2020-supplement

Solid Earth
Open Access

Supplement of

Can subduction initiation at a transform fault be spontaneous?

Diane Arcay et al.

Correspondence to: Diane Arcay (diane.arcay@umontpellier.fr)

The supplementary material contains:

- Additional data (Sect. S1):

  1. the whole simulation list (Table S1 in which experiments are ranked as a function of plate age pair and Table S2 p. 8 in which simulations are gathered as a function of the simulated tectonic behavior);
  2. the graph illustrating the relationship between the brittle parameter, γ, in eq. 1 and the coefficient of internal friction (f_s, Fig. S1) p. 15,
  3. the regime diagrams of deformation as a function of the mechanical property combination (γ_c, γ_m, ρ_c, ρ_{TF}, E_a^c, L_w) showing the simulations used to define regime boundaries, either when OPS is not modeled (Fig. S2 p. 16) or when OPS occurs (Fig. S3 p. 16).

- the estimate of plate bending length L_0 when the oceanic crust is assumed to be weak, and the regime diagram of plate deformation as a function of the weakening extent L_w (Sect. S2 p. 18, Fig. S4 p. 19 and S5) p. 20,
- the results of extra experiments performed to precise the condition of OPS triggering (Sect. S3 p. 21),
- how the different modes of OPS initiation are related to the YP age and thickness (Sect. S4 p. 23, Fig. S7 p. 24 and S8 p. 25),
- the estimate of the strength reduction in the lithospheric mantle necessary to achieve OPS (Sect. S5 p. 23).

S1 Additionnal data

Table S1: Complete simulation list, presented as a function of the plate age pair. *(continued on next pages)*

Run	A_y vs A_o (Myr, Myr)	γ_{TF}/γ_c or γ_c (if 2=3)[a]	γ_m	ρ_c/ρ_{TF}[b] (kg.m^{-3})	E_a^c (kJ/mol)	L_w[c] (A_y; A_o) (km; km)	Specific test	Bottom B.C.	Result
S1a	0 vs 2	0.0005	1.6	3300	360	1100	-	open	OPS-mode 2
S1b	0 vs 2	0.05	1.6	3300	360	0	-	open	YPVSI
S1c	0 vs 2	0.05	1.6	3300	185	0	-	open	YP dripping
S2a	0 vs 5	0.0005	1.6	3300	360	1100	-	open	OPS-mode 2
S2b	0 vs 5	0.0005	0.05	3300	360	1100	-	open	OPS-mode 2
S2c	0 vs 5	0.0005/0.05	1.6	3300	360	50	-	closed	OPS-mode 2
S2d	0 vs 5	0.05	1.6	3300	360	0	-	open	YPVSI
S2e	0 vs 5	0.05	1.6	3300	185	0	-	open	YP dripping
S2f	0 vs 5	0.0005/0.05	1.6	2920/2920	360	TF only[d]	-	closed	cooling
S3a	0 vs 10	0.0005	1.6	3300	360	1100	-	open	OPS-mode 1
S3b	0 vs 10	0.0005	0.05	3300	360	1100	-	open	OPS-mode 1
S3c	0 vs 10	0.05	1.6	3300	360	0	-	open	YPVSI
S3d	0 vs 10	0.05	1.6	3300	185	0	-	open	YP dripping
S4a	0 vs 15	0.0005	1.6	3300	360	1100	-	open	OPS-mode 1
S4b	0 vs 15	0.0005	0.05	3300	360	1100	-	open	OPS-mode 1
S4c	0 vs 15	0.05	1.6	3300	360	0	-	open	YPVSI
S4d	0 vs 15	0.05	1.6	3300	185	0	-	open	YP dripping
S5a	0 vs 20	0.0005	1.6	3300	360	1100	-	open	OPS-mode 1
S5b	0 vs 20	0.0005/0.05	1.6	3300	360	50	-	closed	OPS-mode 2
S5c	0 vs 20	0.05	1.6	3300	360	0	-	open	YPVSI
S5d	0 vs 20	0.05	1.6	3300	185	0	-	open	YP dripping
S6a	0 vs 30	0.0005	1.6	3300	360	1100	-	open	OPS-mode 1

continued on the next page...

. . . continued

Run	A_y,A_o	γ_{TF}/γ_c	γ_m	ρ_c/ρ_{TF}	E_a^c	L_w (A_y; A_o)	Test	Bottom BC	Result
S6b	0 vs 30	0.05	1.6	3300	185	0	-	open	YP dripping
S7a	0 vs 40	0.0005	1.6	3300	360	1100	-	open	OPS-mode 1
S7b	0 vs 40	0.0005	0.05	3300	360	1100	-	open	OPS-mode 1
S7c	0 vs 40	0.0005/0.05	1.6	3300	360	TF only [d]	-	closed	cooling
S7d	0 vs 40	0.0005/0.05	1.6	3300	360	50	-	closed	YPVSI
S7e	0 vs 40	0.05	1.6	3300	360	0	-	open	YPVSI
S7f	0 vs 40	0.05	1.6	3300	185	0	-	open	YP dripping
S8a	0 vs 50	0.0005	1.6	3300	360	1100	-	open	OPS-mode 1
S8b	0 vs 50	0.05	1.6	3300	360	0	-	open	YPVSI
S9a	0 vs 60	0.0005	1.6	3300	360	1100	-	open	OPS-mode 1
S9b	0 vs 60	0.0005/0.05	1.6	3300	360	50	-	closed	YPVSI
S10a	0 vs 80	0.0005	1.6	3300	360	1100	-	open	OPS-mode 1
S10b	0 vs 80	0.0005/0.05	1.6	3300	360	TF only [d]	-	closed	cooling
S10c	0 vs 80	0.05	1.6	3300	360	0	-	open	YPVSI
S10d	0 vs 80	0.0005/0.05	1.6	3300	360	50	-	closed	YPVSI
S11a	0 vs 100	0.0005	1.6	3300	360	1100	-	open	OPS-mode 1
S11b	0 vs 100	0.0005/0.05	1.6	3300	360	TF only [d]	-	closed	cooling
S11c	0 vs 100	0.05	1.6	3300	360	0	-	open	cooling
S12a	0 vs 120	0.0005/0.05	1.6	3300	360	TF only [d]	-	closed	cooling
S12b	0 vs 120	0.0005	1.6	3300	360	1100	-	closed	OPS-mode 1
S13a	0 vs 130	0.05	1.6	3300	360	0	-	open	cooling
S14a	2 vs 5	0.05	1.6	3300	360	0	-	open	cooling
S14b	2 vs 5	0.05	1.6	3300	360	0	-	open	cooling
S14c	2 vs 5	0.0005	1.6	3300	360	1100	-	open	OPS-mode 2, SB
S14d	2 vs 5	0.0005	1.6	3300	360	1100	tw=11km	open	OPS-mode 2, SB
S14e	2 vs 5	0.05	1.6	3300	185	0	-	open	OPS-mode 2, SB
S14f	2 vs 5	0.0005	1.6	3300	360	1100;0	-	open	YPS
S14g	2 vs 5	0.0005	1.6	3300	360	TF only [d]	-	open	cooling
S14h	2 vs 5	0.05	1.6	3300	360	0	ΔT_p =250^{o}C	open	YP dripping
S14i	2 vs 5	0.0005	1.6	3300	360	17;42	-	open	OPS-mode 2
S14j	2 vs 5	0.0005	1.6	3300	360	8.5;20	-	open	OPS-mode 2
S14k	2 vs 5	0.0005	1.6	3300	360	4.3;10	-	open	OPS-mode 2
S14l	2 vs 5	0.0005	1.6	3300	360	2.2;5	-	open	Close to OPS
S14m	2 vs 5	0.0005/0.05	1.6	3300	360	50	-	closed	OPS-mode 2
S14n	2 vs 5	0.0005/0.05	1.6	2920/3300	360	50	-	closed	Double SI
S14o	2 vs 5	0.0005/0.05	1.6	2920/2920	360	TF only [d]	-	closed	cooling
S14p	2 vs 5	0.0005/0.05	1.6	2920/3300	360	TF only [d]	-	closed	YPVSI
S14q	2 vs 5	0.0005/0.01	0.8	3160/3160	360	50	-	closed	Close to OPS
S14r	2 vs 5	0.0005/0.01	0.8	3160/3300	360	50	-	closed	OPS-mode 2
S14s	2 vs 5	0.05/0.0005	1.6	3300	360	TF only [d]	-	closed	YPS then OPS
S15a	2 vs 10	0.05	1.6	3300	185	0	-	open	YP dripping
S15b	2 vs 10	0.0005	1.6	3300	360	1100	-	open	OPS-mode 2
S15c	2 vs 10	0.0005/0.05	1.6	3300	360	1100	-	closed	Close to OPS
S15d	2 vs 10	0.0005	1.6	3300	360	0;1100	-	open	cooling
S15e	2 vs 10	0.0005	1.6	3300	360	1100;0	-	open	cooling
S15f	2 vs 10	0.0005/0.05	1.6	3300	360	TF only [d]	-	closed	YPVSI
S15g	2 vs 10	0.05	1.6	2920/3300	185	1100	-	closed	YPVSI
S15h	2 vs 10	0.05	1.6	2920/3300	360	TF only [d]	ΔT_p =250^{o}C	open	YPVSI
S15i	2 vs 10	0.0005/0.01	0.8	3160/3160	360	50	-	closed	Close to OPS

continued on the next page. . .

. . . continued

Run	A_y,A_o	γ_{TF}/γ_c	γ_m	ρ_c/ρ_{TF}	E_a^c	L_w (A_y;A_o)	Test	Bottom BC	Result
S15j	2 vs 10	0.0005/0.01	0.8	3160/3300	360	50	-	closed	OPS-mode 2
S16a	2 vs 20	0.0005/0.05	1.6	3300	360	50	-	closed	Close to OPS
S16b	2 vs 20	0.0005/0.05	1.6	2920/3300	360	50	-	closed	YPS
S16c	2 vs 20	0.0005/0.05	1.6	2920/2920	360	TF only [d]	-	closed	YP retreat
S16d	2 vs 20	0.0005/0.05	1.6	2920/3300	360	TF only [d]	-	closed	YPVSI
S16e	2 vs 20	0.05	1.6	3300	360	0	-	open	cooling
S16f	2 vs 20	0.0005/0.01	0.6	3160/3160	360	50	-	closed	OPS-mode 2
S16g	2 vs 20	0.0005/0.01	0.8	3160/3160	360	50	-	closed	OPS-mode 2
S17a	2 vs 40	0.05	1.6	3300	360	0	-	open	cooling
S17b	2 vs 40	0.05	1.6	3300	360	0	-	open	YPVSI
S17c	2 vs 40	0.0005	1.6	3300	360	1100	-	open	OPS-mode 2
S17d	2 vs 40	0.05	1.6	3300	185	0	-	open	YP dripping
S17e	2 vs 40	0.0005	1.6	3300	360	1100	-	open	OPS-mode 2
S17f	2 vs 40	0.05	1.6	3300	185	0	-	open	YP dripping
S17g	2 vs 40	0.0005	1.6	3300	360	0;1100	-	open	Close to OPS
S17h	2 vs 40	0.0005	1.6	3300	360	1100;0	-	open	YPVSI
S17i	2 vs 40	0.0005	1.6	3300	360	TF only [d]	-	open	cooling
S17j	2 vs 40	0.05	1.6	3300	360	0	ΔT_p =250^{o}C	open	YP dripping
S17k	2 vs 40	0.0005/0.05	1.6	3300	360	TF only [d]	-	closed	cooling
S17l	2 vs 40	0.0005/0.05	1.6	3300	360	1100	-	closed	cooling
S17m	2 vs 40	0.0005	1.6	2920/3300	360	TF only [d]	-	closed	Close to OPS
S17n	2 vs 40	0.0005	1.6	3300	360	TF only [d]	-	closed	OPS-mode 2
S17o	2 vs 40	0.0005/0.05	1.6	3300	360	50	-	closed	YPVSI
S17p	2 vs 40	0.0005/0.05	1.6	2920/2920	360	TF only [d]	-	closed	YP retreat
S17q	2 vs 40	0.0005/0.05	1.6	2920/3300	360	TF only [d]	-	closed	YPVSI
S17r	2 vs 40	0.0005/0.05	1.6	2920/3300	360	50	-	closed	YPVSI
S17s	2 vs 40	0.0005/0.05	1.6	3300	360	TF only [d]	-	closed	YPVSI
S17t	2 vs 40	0.0005/0.01	0.6	3160/3160	360	50	-	closed	OPS-mode 2
S17u	2 vs 40	0.05/0.0005	1.6	3300	360	TF only [d]	-	closed	YPS
S17v	2 vs 40	0.0005/0.01	0.8	3160/3160	360	50	-	closed	OPS-mode 2
S18a	2 vs 80	0.05	1.6	3300	360	0	-	open	YPVSI
S18a2	2 vs 80	0.05	1.6	3300	360	0	tw=11km	open	YPVSI
S18b	2 vs 80	0.0005	1.6	3300	360	1100	-	open	OPS-mode 2
S18b2	2 vs 80	0.0005	1.6	3300	360	1100	tw=11km	open	OPS-mode 2
S18b3	2 vs 80	0.0005	1.6	3300	360	1100	tw=30 km	open	OPS-mode 2
S18b4	2 vs 80	0.0005	1.6	3300	360	1100	tw=50 km	open	OPS-mode 2
S18b5	2 vs 80	0.0005	1.6	3300	360	1100	tw=70 km	open	OPS-mode 2
S18c	2 vs 80	0.005	1.6	3300	360	1100	-	open	cooling
S18d	2 vs 80	0.0007	1.6	3300	360	1100	-	open	OPS-mode 2
S18e	2 vs 80	0.001	1.6	3300	360	1100	-	open	OPS-mode 2
S18f	2 vs 80	0.05	1.6	3300	185	0	-	open	YP dripping
S18g	2 vs 80	0.05	1.6	3300	185	0	-	open	YP dripping
S18h	2 vs 80	0.0005	1.6	3300	360	0;1100	-	open	Close to OPS
S18i	2 vs 80	0.0005	1.6	3300	360	1100;0	-	open	YP dripping
S18j	2 vs 80	0.0005	1.6	3300	360	TF only [d]	-	open	cooling
S18k	2 vs 80	0.05	1.6	3300	360	0	ΔT_p =250^{o}C	open	YP dripping
S18m	2 vs 80	0.0005	1.6	2920/3300	360	TF only [d]	-	closed	Close to OPS
S18n	2 vs 80	0.0005/0.05	1.6	3300	360	TF only [d]	-	closed	cooling
S18o	2 vs 80	0.0005/0.05	0.6	3300	360	TF only [d]	-	closed	cooling

continued on the next page. . .

. . . continued

Run	A_y,A_o	γ_{TF}/γ_c	γ_m	ρ_c/ρ_{TF}	E_a^c	L_w ($A_y;A_o$)	Test	Bottom BC	Result
S18p	2 vs 80	0.0005	0.6	2920/3300	360	TF only [d]	-	closed	OPS-mode 2
S18q	2 vs 80	0.0005/0.05	1.6	3300	360	50	-	closed	YPVSI
S18r	2 vs 80	0.0005/0.05	1.6	2920/2920	360	TF only [d]	-	closed	YP retreat
S18s	2 vs 80	0.0005/0.05	1.6	2920/3300	360	TF only [d]	-	closed	YPVSI
S18t	2 vs 80	0.0005/0.05	1.6	3300	360	50	-	closed	YP retreat
S18u	2 vs 80	0.0005/0.05	1.6	3300	360	TF only [d]	-	closed	YPVSI
S19a	2 vs 100	0.05	1.6	3300	360	0	-	open	YPVSI
S19b	2 vs 100	0.0005	1.6	3300	360	1100	-	open	OPS-mode 2
S20a	2 vs 120	0.0005	1.6	3300	360	1100	-	open	OPS-mode 2
S21a	5 vs 10	0.0005	0.1	3300	360	1100	-	open	OPS-mode 1
S21b	5 vs 10	0.0005/0.05	1.6	2920/3300	360	50	-	closed	YPVSI
S21c	5 vs 10	0.0005/0.05	1.6	3300	360	50	-	closed	YPVSI
S21d	5 vs 10	0.0005/0.05	1.6	3300	360	TF only [d]	-	closed	cooling
S22a	5 vs 15	0.05	1.6	3300	360	0	-	open	cooling
S22b	5 vs 15	0.05	1.6	3300	360	0	-	open	cooling
S22c	5 vs 15	0.0005	1.6	3300	360	1100	-	open	cooling
S22d	5 vs 15	0.00005	1.6	3300	360	1100	ttw=11 km	open	cooling
S22e	5 vs 15	0.05	1.6	3300	185	0	-	open	cooling
S22f	5 vs 15	0.0005	1.6	3300	360	1100	-	open	cooling
S22g	5 vs 15	0.00005	1.6	3300	185	1100	-	open	cooling
S22h	5 vs 15	0.0005	1.6	3300	360	1100	$\nu_{ref}/5$	open	cooling
S22i	5 vs 15	0.0005	0.2	3300	360	1100	-	open	cooling
S22j	5 vs 15	0.0005	0.1	3300	360	1100	-	open	OPS-mode 2, SB
S22k	5 vs 15	0.0005	0.05	3300	360	1100	-	open	OPS-mode 2, SB
S22l	5 vs 15	0.05	1.6	3300	185	0	-	open	cooling
S22n	5 vs 15	0.0005	1.6	3300	360	0;1100	-	open	cooling
S22o	5 vs 15	0.00005	1.6	3300	360	0;1100	-	open	cooling
S22p	5 vs 15	0.0005	1.6	3300	360	1100;0	-	open	cooling
S22q	5 vs 15	0.00005	1.6	3300	360	1100;0	-	open	cooling
S22r	5 vs 15	0.0005	1.6	3300	360	TF only [d]	-	open	cooling
S22s	5 vs 15	0.05	1.6	3300	360	0	ΔT_p =250^{o}C	open	cooling
S22t	5 vs 15	0.00005	1.6	3300	360	1100	TFW=20 km	open	cooling
S23a	5 vs 20	0.0005	1.6	3300	360	1100	-	open	cooling
S23b	5 vs 20	0.05	1.6	3300	185	0	-	open	cooling
S23c	5 vs 20	0.0005/0.05	1.6	3300	360	50	-	closed	YPVSI
S23d	5 vs 20	0.0005/0.05	1.6	2920/3300	360	50	-	closed	YPVSI
S23e	5 vs 20	0.0005/0.05	1.6	2920/2920	360	TF only [d]	-	closed	YPS
S23f	5 vs 20	0.0005/0.05	1.6	2920/3300	360	TF only [d]	-	closed	YPVSI
S24a	5 vs 30	0.0005	1.6	3300	360	1100	-	open	Close to OPS
S24b	5 vs 30	0.05	1.6	3300	185	0	-	open	cooling
S25a	5 vs 35	0.0005	1.6	3300	360	1100	-	open	Close to OPS
S25b	5 vs 35	0.0005	1.6	3300	360	1100	E_a^m =390 kJ/mol	open	Close to OPS
S25c	5 vs 35	0.0005	1.6	3300	360	1100	E_a^m =360 kJ/mol	open	Close to OPS
S25d	5 vs 35	0.0005	1.6	3300	360	1100	E_a^m =300 kJ/mol	open	Close to OPS
S26a	5 vs 40	0.0005	1.6	3300	360	1100	-	open	OPS-mode 1
S26ai	5 vs 40	0.0001	1.6	3300	360	1100	-	open	OPS-mode 1
S26aii	5 vs 40	0.005	1.6	3300	360	1100	-	open	cooling
S26aiii	5 vs 40	0.001	1.6	3300	360	1100	-	open	cooling
S26b	5 vs 40	0.0005/0.05	1.6	3300	360	50	-	closed	YPVSI

continued on the next page. . .

...continued

Run	A_y,A_o	γ_{TF}/γ_c	γ_m	ρ_c/ρ_{TF}	E_a^c	L_w (A_y; A_o)	Test	Bottom BC	Result
S26c	5 vs 40	0.0005/0.05	1.6	2920/2920	360	TF only [d]	-	closed	YPS
S26d	5 vs 40	0.0005/0.05	0.05	2920/3300	360	50	-	closed	YPVSI
S26e	5 vs 40	0.0005/0.05	1.6	3300	360	TF only [d]	-	closed	cooling
S26f	5 vs 40	0.0005	1.6	3300	360	1100	SWL	open	OPS-mode 1
S26fi	5 vs 40	0.0001	1.6	3300	360	1100	SWL	open	OPS-mode 1
S26fii	5 vs 40	0.005	1.6	3300	360	1100	SWL	open	OPS-mode 1
S26fiii	5 vs 40	0.001	1.6	3300	360	1100	SWL	open	OPS-mode 1
S26fiv	5 vs 40	0.01	1.6	3300	360	1100	SWL	open	Close to OPS
S26fv	5 vs 40	0.025	1.6	3300	360	1100	SWL	open	cooling
S26fvi	5 vs 40	0.05	1.6	3300	360	1100	SWL	open	cooling
S27a	5 vs 50	0.0005	1.6	3300	360	1100	-	open	OPS-mode 1
S27b	5 vs 50	0.05	1.6	3300	185	0	-	open	cooling
S27c	5 vs 50	0.0005	1.6	3300	360	42;260	-	open	OPS-mode 1
S27d	5 vs 50	0.0005	1.6	3300	360	20;142	-	open	Close to OPS
S27e	5 vs 50	0.0005	1.6	3300	360	10;71	-	open	cooling
S27f	5 vs 50	0.05	1.6	3300	360	0	-	open	cooling
S28a	5 vs 80	0.0005/0.05	1.6	3300	360	50	-	closed	YPVSI
S28c	5 vs 80	0.0005/0.05	1.6	2920/3300	360	50	-	closed	cooling
S28d	5 vs 80	0.0005/0.05	1.6	2920/3300	360	TF only [d]	-	closed	YPVSI
S28e	5 vs 80	0.0005/0.05	1.6	2920/2920	360	TF only [d]	-	closed	YPS
S28f	5 vs 80	0.0005/0.05	1.6	3300	360	TF only [d]	-	closed	cooling
S29a	5 vs 100	0.0005	1.6	3300	360	1100	-	open	OPS-mode 1
S29b	5 vs 120	0.0005	1.6	3300	360	1100	-	open	Close to OPS
S30a	7 vs 20	0.0005	0.1	3300	360	1100	-	open	cooling
S30b	7 vs 20	0.0005	0.05	3300	360	1100	-	open	cooling
S31a	7 vs 30	0.0005	0.1	3300	360	1100	-	open	OPS-mode 1
S31-2a	7 vs 60	0.0005	0.1	3300	360	1100	-	open	cooling
S32a	7 vs 70	0.0005	1.6	3300	360	1100	-	open	cooling
S32b	7 vs 70	0.0005	1.6	3300	360	1100	E_a^m =390 kJ/mol	open	Close to OPS
S32c	7 vs 70	0.0005	1.6	3300	360	1100	E_a^m =360 kJ/mol	open	Close to OPS
S32d	7 vs 70	0.0005	1.6	3300	360	1100	E_a^m =300 kJ/mol	open	Close to OPS
S33a	7 vs 80	0.0005	1.6	3300	360	1100	-	open	Close to OPS
S33b	7 vs 80	0.0005	1.6	3300	360	1100	E_a^m =390 kJ/mol	open	Close to OPS
S33c	7 vs 80	0.0005	1.6	3300	360	1100	E_a^m =360 kJ/mol	open	Close to OPS
S33d	7 vs 80	0.0005	1.6	3300	360	1100	E_a^m =300 kJ/mol	open	Close to OPS
S34a	7 vs 90	0.0005	1.6	3300	360	1100	-	open	Close to OPS
S34b	7 vs 90	0.0005	0.1	3300	360	1100	-	open	OPS-mode1, SB
S34c	7 vs 90	0.0005	1.6	3300	360	1100	E_a^m =390 kJ/mol	open	Close to OPS
S34d	7 vs 90	0.0005	1.6	3300	360	1100	E_a^m =360 kJ/mol	open	Close to OPS
S34e	7 vs 90	0.0005	1.6	3300	360	1100	E_a^m =300 kJ/mol	open	OPS-mode 1
S35a	7 vs 100	0.0005	1.6	3300	360	1100	-	open	OPS-mode 1
S35b	7 vs 120	0.0005	1.6	3300	360	1100	-	open	Close to OPS
S36a	10 vs 20	0.0005	0.05	3300	360	1100	-	open	cooling
S36b	10 vs 20	0.0005/0.05	1.6	2920/2920	360	TF only [d]	-	closed	YPS
S36c	10 vs 20	0.0005/0.05	1.6	2920/3300	360	50	-	closed	cooling
S37a	10 vs 40	0.05	1.6	3300	360	0	-	open	cooling
S37b	10 vs 40	0.0005	1.6	3300	360	1100	-	open	cooling
S37b2	10 vs 40	0.0005	1.6	3300	360	1100	$\nu_{ref}/10$	open	cooling
S37c	10 vs 40	0.0005	0.4	3300	360	1100	-	open	cooling

continued on the next page...

. . . continued

Run	A_y,A_o	γ_{TF}/γ_c	γ_m	ρ_c/ρ_{TF}	E_a^c	L_w ($A_y;A_o$)	Test	Bottom BC	Result
S37d	10 vs 40	0.0005	0.1	3300	360	1100	-	open	Close to OPS
S37e	10 vs 40	0.0005	0.075	3300	360	1100	-	open	Close to OPS
S37f	10 vs 40	0.0005	0.05	3300	360	1100	-	open	OPS-mode 1
S37g	10 vs 40	0.05	1.6	3300	185	1100	-	open	cooling
S37h	10 vs 40	0.0005	0.05	3300	360	0;1100	-	open	Close to OPS
S37i	10 vs 40	0.0005	0.05	3300	360	85;238	-	open	cooling
S37j	10 vs 40	0.0005	0.05	3300	360	43;119	-	open	cooling
S37k	10 vs 40	0.0005	0.05	3300	360	21;60	-	open	cooling
S37l	10 vs 40	0.0005/0.05	0.05	3300	360	50	-	closed	cooling
S37m	10 vs 40	0.05	1.6	3300	185	0	-	open	cooling
S37n	10 vs 40	0.0005	1.6	3300	360	0;1100	-	open	cooling
S37o	10 vs 40	0.0005	1.6	3300	360	1100;0	-	open	cooling
S37p	10 vs 40	0.0005	1.6	3300	360	TF only [d]	-	open	cooling
S37q	10 vs 40	0.05	1.6	3300	360	0	ΔT_p =250^{o}C	open	cooling
S37r	10 vs 40	0.0005	1.6	3300	360	1100	TFW=20km	open	cooling
S37s	10 vs 40	0.00005	1.6	3300	360	1100	TFW=20 km	open	cooling
S37t	10 vs 40	0.00005	1.6	3300	360	1100	-	open	cooling
S37v	10 vs 40	0.05	1.6	3300	150	0	-	open	cooling
S37w	10 vs 40	0.0005/0.05	0.05	2920/2920	360	TF only [d]	-	closed	YPS
S37x	10 vs 40	0.0005/0.05	0.05	2920/3300	360	TF only [d]	-	closed	cooling
S37y	10 vs 40	0.0005/0.05	0.05	2920/3300	360	50	-	closed	cooling
S37z	10 vs 40	0.0005/0.05	1.6	3300	360	TF only [d]	-	closed	cooling
S38a	10 vs 50	0.0005	0.1	3300	360	1100	-	open	OPS-mode 1
S39a	10 vs 60	0.0005	1.6	3300	360	1100	-	open	cooling
S39b	10 vs 60	0.0005	0.1	3300	360	1100	-	open	OPS-mode 1
S40a	10 vs 80	0.0005	1.6	3300	360	1100	-	open	cooling
S40b	10 vs 80	0.0005/0.05	1.6	3300	360	50	-	closed	cooling
S40c	10 vs 80	0.0005/0.05	1.6	2920/2920	360	TF only [d]	-	closed	YPS
S41a	10 vs 100	0.0005	1.6	3300	360	1100	-	open	cooling
S42a	10 vs 130	0.0005	1.6	3300	360	1100	-	open	cooling
S43a	10 vs 140	0.0005	1.6	3300	360	1100	-	open	Close to OPS
S44a	10 vs 150	0.0005	1.6	3300	360	1100	-	open	Close to OPS
S45a	15 vs 30	0.0005	0.05	3300	360	1100	-	open	cooling
S46a	15 vs 40	0.0005	0.05	3300	360	1100	-	open	Close to OPS
S46b	15 vs 40	0.0005/0.05	1.6	2920/2920	360	TF only [d]	-	closed	YPS
S47a	15 vs 60	0.0005	0.1	3300	360	1100	-	open	OPS-mode 1
S47b	15 vs 60	0.0005	0.08	3300	360	1100	-	open	OPS-mode 1
S47c	15 vs 60	0.0005	0.06	3300	360	1100	-	open	OPS-mode 1
S47d	15 vs 60	0.0005	0.05	3300	360	1100	-	open	OPS-mode 1
S48a	15 vs 80	0.0005/0.05	1.6	2920/2920	360	TF only [d]	-	closed	YPS
S49a	20 vs 40	0.05	1.6	3300	360	0	-	open	cooling
S49b	20 vs 40	0.0005	1.6	3300	360	1100	ttw=11 km	open	cooling
S49c	20 vs 40	0.00005	1.6	3300	360	1100	-	open	cooling
S49d	20 vs 40	0.0005	1.6	3300	360	1100	-	open	cooling
S49e	20 vs 40	0.00005	1.6	3300	360	1100	-	open	cooling
S49f	20 vs 40	0.0005	1.6	3300	360	1100	$\nu_{ref}/10$	open	cooling
S49g	20 vs 40	0.0005	0.05	3300	360	1100	-	open	cooling
S49h	20 vs 40	0.0005	0.005	3300	360	1100	-	open	OPS, SB, YPD
S49i	20 vs 40	0.0005	0.005	3300	360	151;238	-	open	OPS-mode 1 , SB, YPD

continued on the next page. . .

. . . continued

Run	A_y,A_o	γ_{TF}/γ_c	γ_m	ρ_c/ρ_{TF}	E_a^c	L_w ($A_y;A_o$)	Test	Bottom BC	Result
S49j	20 vs 40	0.0005	0.005	3300	360	76;119	-	open	OPS-mode 1, SB, YPD
S49k	20 vs 40	0.0005	0.005	3300	360	38;60	-	open	OPS-mode 1
S49l	20 vs 40	0.0005	0.005	3300	360	19;30	-	open	OPS-mode 1
S49m	20 vs 40	0.0005/0.05	1.6	3300	360	50	-	closed	cooling
S49n	20 vs 40	0.0005/0.05	1.6	2920/2920	360	TF only [d]	-	closed	cooling
S49o	20 vs 40	0.0005/0.05	1.6	2920/2920	360	TF only [d]	-	closed	cooling
S49p	20 vs 40	0.00005	1.6	3300	360	1100	-	open	cooling
S49q	20 vs 40	0.05	1.6	3300	185	0	-	open	cooling
S49r	20 vs 40	0.05	1.6	3300	120	0	-	open	cooling
S49s	20 vs 40	0.05	1.6	3300	185	0	-	open	cooling
S49t	20 vs 40	0.05	1.6	3300	120	0	-	open	cooling
S49v	20 vs 40	0.00005	1.6	3300	360	1100	-	open	cooling
S49w	20 vs 40	0.0005	1.6	3300	360	1100	-	open	cooling
S49y	20 vs 40	0.0005	1.6	3300	360	1100	-	open	cooling
S49z	20 vs 40	0.05	1.6	3300	360	0	ΔT_p =250^{o}C	open	cooling
S50a	20 vs 60	0.0005	0.1	3300	360	1100	-	open	cooling
S50b	20 vs 60	0.0005	0.05	3300	360	1100	-	open	Close to OPS
S51a	20 vs 80	0.0005	1.6	3300	360	1100	-	open	cooling
S51b	20 vs 80	0.0005	0.1	3300	360	1100	-	open	Close to OPS
S51c	20 vs 80	0.0005	0.08	3300	360	1100	-	open	Close to OPS
S51d	20 vs 80	0.0005	0.06	3300	360	1100	-	open	OPS-mode 1
S51e	20 vs 80	0.0005	0.05	3300	360	1100	-	open	OPS-mode 1
S51f	20 vs 80	0.0005/0.05	1.6	3300	360	50	-	closed	cooling
S52a	20 vs 100	0.0005	1.6	3300	360	1100	-	open	cooling
S52b	20 vs 100	0.0005	0.1	3300	360	1100	-	open	OPS-mode 1
S53a	20 vs 130	0.0005	0.1	3300	360	1100	-	open	OPS-mode 1, SB
S54a	25 vs 40	0.0005	0.05	3300	360	1100	-	open	cooling
S55a	25 vs 60	0.0005	0.05	3300	360	1100	-	open	cooling
S56a	25 vs 80	0.0005	0.05	3300	360	1100	-	open	Close to OPS
S57a	25 vs 100	0.0005	0.05	3300	360	1100	-	open	OPS-mode 1
S57b	25 vs 100	0.0005	0.075	3300	360	1100	-	open	Close to OPS

[a]If one value only is indicated, the oceanic crust ③ in Fig. 2 is assumed to have the same brittle parameter as the one of the weak material forming domains ① and ②. [b]If only one value indicated, then $\rho_c = \rho_{TF}$. [c]If one value only indicated, L_w is identical on both plates. [d]The weak material is imposed to form the fault zone ① only (Fig. 2). "tw": thermal transition width at the plate boundary. "TFW": TF width, filled by the weak material 1. ΔT_p: temperature anomaly within the plume head. ν_{ref}: reference viscosity at the lithosphere-asthenosphere boundary at simulation start (2.74×10^{19} Pa.s). SWL: sticky water layer inserted at the box surface. OPS: older plate sinking. YPVSI: YP vertical subduction initiation (as in Fig. 4-6). YP retreat: backward drift of the younger plate (Fig. 4-3). YPS: younger plate sinking (sketched in Fig. 4-4b). Double SI: double subduction initiation (Fig. 4-5). SB: slab break-off. YPD: young plate dragging and sinking into the mantle.

Table S2: Complete simulation list, as in Table S1 but here compiled as a function of the deformation regime. Footnotes and acronyms are defined in Table S1 caption. *(continued on next pages)*

Run	A_y vs A_o (Myr, Myr)	γ_{TF}/γ_c or γ_c (if ②=③)[a]	γ_m	ρ_c/ρ_{TF}[b] (kg.m^{-3})	E_a^c (kJ/mol)	L_w[c] $(A_y; A_o)$ (km; km)	Specific test	Bottom B.C.	Result
S2f	0 vs 5	0.0005/0.05	1.6	2920/2920	360	TF only [d]	-	closed	cooling
S7c	0 vs 40	0.0005/0.05	1.6	3300	360	TF only [d]	-	closed	cooling
S10b	0 vs 80	0.0005/0.05	1.6	3300	360	TF only [d]	-	closed	cooling
S11b	0 vs 100	0.0005/0.05	1.6	3300	360	TF only [d]	-	closed	cooling
S11c	0 vs 100	0.05	1.6	3300	360	0	-	open	cooling
S12a	0 vs 120	0.0005/0.05	1.6	3300	360	TF only [d]	-	closed	cooling
S13a	0 vs 130	0.05	1.6	3300	360	0	-	open	cooling
S14a	2 vs 5	0.05	1.6	3300	360	0	-	open	cooling
S14b	2 vs 5	0.05	1.6	3300	360	0	-	open	cooling
S14g	2 vs 5	0.0005	1.6	3300	360	TF only [d]	-	open	cooling
S14o	2 vs 5	0.0005/0.05	1.6	2920/2920	360	TF only [d]	-	closed	cooling
S15d	2 vs 10	0.0005	1.6	3300	360	" 0;1100 "	-	open	cooling
S15e	2 vs 10	0.0005	1.6	3300	360	" 1100;0 "	-	open	cooling
S16e	2 vs 20	0.05	1.6	3300	360	0	-	open	cooling
S17a	2 vs 40	0.05	1.6	3300	360	0	-	open	cooling
S17i	2 vs 40	0.0005	1.6	3300	360	TF only [d]	-	open	cooling
S17k	2 vs 40	0.0005/0.05	1.6	3300	360	TF only [d]	-	closed	cooling
S17l	2 vs 40	0.0005/0.05	1.6	3300	360	1100	-	closed	cooling
S18c	2 vs 80	0.005	1.6	3300	360	1100	-	open	cooling
S18j	2 vs 80	0.0005	1.6	3300	360	TF only [d]	-	open	cooling
S18n	2 vs 80	0.0005/0.05	1.6	3300	360	TF only [d]	-	closed	cooling
S18o	2 vs 80	0.0005/0.05	0.6	3300	360	TF only [d]	-	closed	cooling
S21d	5 vs 10	0.0005/0.05	1.6	3300	360	TF only [d]	-	closed	cooling
S22a	5 vs 15	0.05	1.6	3300	360	0	-	open	cooling
S22b	5 vs 15	0.05	1.6	3300	360	0	-	open	cooling
S22c	5 vs 15	0.0005	1.6	3300	360	1100	-	open	cooling
S22d	5 vs 15	0.00005	1.6	3300	360	1100	ttw=11 km	open	cooling
S22e	5 vs 15	0.05	1.6	3300	185	0	-	open	cooling
S22f	5 vs 15	0.0005	1.6	3300	360	1100	-	open	cooling
S22g	5 vs 15	0.00005	1.6	3300	185	1100	-	open	cooling
S22h	5 vs 15	0.0005	1.6	3300	360	1100	$\nu_{ref}/5$	open	cooling
S22i	5 vs 15	0.0005	0.2	3300	360	1100	-	open	cooling
S22l	5 vs 15	0.05	1.6	3300	185	0	-	open	cooling
S22n	5 vs 15	0.0005	1.6	3300	360	" 0;1100 "	-	open	cooling
S22o	5 vs 15	0.00005	1.6	3300	360	" 0;1100 "	-	open	cooling
S22p	5 vs 15	0.0005	1.6	3300	360	" 1100;0 "	-	open	cooling
S22q	5 vs 15	0.00005	1.6	3300	360	" 1100;0 "	-	open	cooling
S22r	5 vs 15	0.0005	1.6	3300	360	TF only [d]	-	open	cooling
S22s	5 vs 15	0.05	1.6	3300	360	0	ΔT_p =250^{o}C	open	cooling
S22t	5 vs 15	0.00005	1.6	3300	360	1100	TFW=20 km	open	cooling
S23a	5 vs 20	0.0005	1.6	3300	360	1100	-	open	cooling
S23b	5 vs 20	0.05	1.6	3300	185	0	-	open	cooling
S24b	5 vs 30	0.05	1.6	3300	185	0	-	open	cooling
S26aii	5 vs 40	0.005	1.6	3300	360	1100	-	open	cooling
S26aiii	5 vs 40	0.001	1.6	3300	360	1100	-	open	cooling
S26e	5 vs 40	0.0005/0.05	1.6	3300	360	TF only [d]	-	closed	cooling

continued on the next page…

…continued

Run	A_y,A_o	γ_{TF}/γ_c	γ_m	ρ_c/ρ_{TF}	E_a^c	L_w (A_y; A_o)	Test	Bottom BC	Result
S26fv	5 vs 40	0.025	1.6	3300	360	1100	SWL	open	cooling
S26fvi	5 vs 40	0.05	1.6	3300	360	1100	SWL	open	cooling
S27b	5 vs 50	0.05	1.6	3300	185	0	-	open	cooling
S27e	5 vs 50	0.0005	1.6	3300	360	" 10;71 "	-	open	cooling
S27f	5 vs 50	0.05	1.6	3300	360	0	-	open	cooling
S28c	5 vs 80	0.0005/0.05	1.6	2920/3300	360	50	-	closed	cooling
S28f	5 vs 80	0.0005/0.05	1.6	3300	360	TF only [d]	-	closed	cooling
S30a	7 vs 20	0.0005	0.1	3300	360	1100	-	open	cooling
S30b	7 vs 20	0.0005	0.05	3300	360	1100	-	open	cooling
S31-2a	7 vs 60	0.0005	0.1	3300	360	1100	-	open	cooling
S32a	7 vs 70	0.0005	1.6	3300	360	1100	-	open	cooling
S36a	10 vs 20	0.0005	0.05	3300	360	1100	-	open	cooling
S36c	10 vs 20	0.0005/0.05	1.6	2920/3300	360	50	-	closed	cooling
S37a	10 vs 40	0.05	1.6	3300	360	0	-	open	cooling
S37b	10 vs 40	0.0005	1.6	3300	360	1100	-	open	cooling
S37b2	10 vs 40	0.0005	1.6	3300	360	1100	$\nu_{ref}/10$	open	cooling
S37c	10 vs 40	0.0005	0.4	3300	360	1100	-	open	cooling
S37g	10 vs 40	0.05	1.6	3300	185	1100	-	open	cooling
S37i	10 vs 40	0.0005	0.05	3300	360	" 85;238 "	-	open	cooling
S37j	10 vs 40	0.0005	0.05	3300	360	" 43;119 "	-	open	cooling
S37k	10 vs 40	0.0005	0.05	3300	360	" 21;60 "	-	open	cooling
S37l	10 vs 40	0.0005/0.05	0.05	3300	360	50	-	closed	cooling
S37m	10 vs 40	0.05	1.6	3300	185	0	-	open	cooling
S37n	10 vs 40	0.0005	1.6	3300	360	" 0;1100 "	-	open	cooling
S37o	10 vs 40	0.0005	1.6	3300	360	" 1100;0 "	-	open	cooling
S37p	10 vs 40	0.0005	1.6	3300	360	TF only [d]	-	open	cooling
S37q	10 vs 40	0.05	1.6	3300	360	0	ΔT_p =250^{o}C	open	cooling
S37r	10 vs 40	0.0005	1.6	3300	360	1100	TFW=20 km	open	cooling
S37s	10 vs 40	0.00005	1.6	3300	360	1100	TFW=20 km	open	cooling
S37t	10 vs 40	0.00005	1.6	3300	360	1100	-	open	cooling
S37v	10 vs 40	0.05	1.6	3300	150	0	-	open	cooling
S37x	10 vs 40	0.0005/0.05	0.05	2920/3300	360	TF only [d]	-	closed	cooling
S37y	10 vs 40	0.0005/0.05	0.05	2920/3300	360	50	-	closed	cooling
S37z	10 vs 40	0.0005/0.05	1.6	3300	360	TF only [d]	-	closed	cooling
S39a	10 vs 60	0.0005	1.6	3300	360	1100	-	open	cooling
S40a	10 vs 80	0.0005	1.6	3300	360	1100	-	open	cooling
S40b	10 vs 80	0.0005/0.05	1.6	3300	360	50	-	closed	cooling
S41a	10 vs 100	0.0005	1.6	3300	360	1100	-	open	cooling
S42a	10 vs 130	0.0005	1.6	3300	360	1100	-	open	cooling
S45a	15 vs 30	0.0005	0.05	3300	360	1100	-	open	cooling
S49a	20 vs 40	0.05	1.6	3300	360	0	-	open	cooling
S49b	20 vs 40	0.0005	1.6	3300	360	1100	ttw=11 km	open	cooling
S49c	20 vs 40	0.00005	1.6	3300	360	1100	-	open	cooling
S49d	20 vs 40	0.0005	1.6	3300	360	1100	-	open	cooling
S49e	20 vs 40	0.00005	1.6	3300	360	1100	-	open	cooling
S49f	20 vs 40	0.0005	1.6	3300	360	1100	$\nu_{ref}/10$	open	cooling
S49g	20 vs 40	0.0005	0.05	3300	360	1100	-	open	cooling
S49m	20 vs 40	0.0005/0.05	1.6	3300	360	50	-	closed	cooling
S49n	20 vs 40	0.0005/0.05	1.6	2920/2920	360	TF only [d]	-	closed	cooling

continued on the next page…

. . . continued

Run	A_y,A_o	γ_{TF}/γ_c	γ_m	ρ_c/ρ_{TF}	E_a^c	L_w ($A_y; A_o$)	Test	Bottom BC	Result
S49o	20 vs 40	0.0005/0.05	1.6	2920/2920	360	TF only [d]	-	closed	cooling
S49p	20 vs 40	0.00005	1.6	3300	360	1100	-	open	cooling
S49q	20 vs 40	0.05	1.6	3300	185	0	-	open	cooling
S49r	20 vs 40	0.05	1.6	3300	120	0	-	open	cooling
S49s	20 vs 40	0.05	1.6	3300	185	0	-	open	cooling
S49t	20 vs 40	0.05	1.6	3300	120	0	-	open	cooling
S49v	20 vs 40	0.00005	1.6	3300	360	1100	-	open	cooling
S49w	20 vs 40	0.0005	1.6	3300	360	1100	-	open	cooling
S49y	20 vs 40	0.0005	1.6	3300	360	1100	-	open	cooling
S49z	20 vs 40	0.05	1.6	3300	360	0	$\Delta T_p = 250^o$C	open	cooling
S50a	20 vs 60	0.0005	0.1	3300	360	1100	-	open	cooling
S51a	20 vs 80	0.0005	1.6	3300	360	1100	-	open	cooling
S51f	20 vs 80	0.0005/0.05	1.6	3300	360	50	-	closed	cooling
S52a	20 vs 100	0.0005	1.6	3300	360	1100	-	open	cooling
S54a	25 vs 40	0.0005	0.05	3300	360	1100	-	open	cooling
S55a	25 vs 60	0.0005	0.05	3300	360	1100	-	open	cooling
S1c	0 vs 2	0.05	1.6	3300	185	0	-	open	YP dripping
S2e	0 vs 5	0.05	1.6	3300	185	0	-	open	YP dripping
S3d	0 vs 10	0.05	1.6	3300	185	0	-	open	YP dripping
S4d	0 vs 15	0.05	1.6	3300	185	0	-	open	YP dripping
S5d	0 vs 20	0.05	1.6	3300	185	0	-	open	YP dripping
S6b	0 vs 30	0.05	1.6	3300	185	0	-	open	YP dripping
S7f	0 vs 40	0.05	1.6	3300	185	0	-	open	YP dripping
S14h	2 vs 5	0.05	1.6	3300	360	0	$\Delta T_p = 250^o$C	open	YP dripping
S15a	2 vs 10	0.05	1.6	3300	185	0	-	open	YP dripping
S17d	2 vs 40	0.05	1.6	3300	185	0	-	open	YP dripping
S17f	2 vs 40	0.05	1.6	3300	185	0	-	open	YP dripping
S17j	2 vs 40	0.05	1.6	3300	360	0	$\Delta T_p = 250^o$C	open	YP dripping
S18f	2 vs 80	0.05	1.6	3300	185	0	-	open	YP dripping
S18g	2 vs 80	0.05	1.6	3300	185	0	-	open	YP dripping
S18i	2 vs 80	0.0005	1.6	3300	360	" 1100;0 "	-	open	YP dripping
S18k	2 vs 80	0.05	1.6	3300	360	0	$\Delta T_p = 250^o$C	open	YP dripping
S16c	2 vs 20	0.0005/0.05	1.6	2920/2920	360	TF only [d]	-	closed	YP retreat
S17p	2 vs 40	0.0005/0.05	1.6	2920/2920	360	TF only [d]	-	closed	YP retreat
S18r	2 vs 80	0.0005/0.05	1.6	2920/2920	360	TF only [d]	-	closed	YP retreat
S18t	2 vs 80	0.0005/0.05	1.6	3300	360	50	-	closed	YP retreat
S14f	2 vs 5	0.0005	1.6	3300	360	" 1100;0 "	-	open	YPS
S16b	2 vs 20	0.0005/0.05	1.6	2920/3300	360	50	-	closed	YPS
S17u	2 vs 40	0.05/0.0005	1.6	3300	360	TF only [d]	-	closed	YPS
S23e	5 vs 20	0.0005/0.05	1.6	2920/2920	360	TF only [d]	-	closed	YPS
S26c	5 vs 40	0.0005/0.05	1.6	2920/2920	360	TF only [d]	-	closed	YPS
S28e	5 vs 80	0.0005/0.05	1.6	2920/2920	360	TF only [d]	-	closed	YPS
S36b	10 vs 20	0.0005/0.05	1.6	2920/2920	360	TF only [d]	-	closed	YPS
S37w	10 vs 40	0.0005/0.05	0.05	2920/2920	360	TF only [d]	-	closed	YPS
S40c	10 vs 80	0.0005/0.05	1.6	2920/2920	360	TF only [d]	-	closed	YPS
S46b	15 vs 40	0.0005/0.05	1.6	2920/2920	360	TF only [d]	-	closed	YPS

continued on the next page. . .

. . . continued

Run	A_y,A_o	γ_{TF}/γ_c	γ_m	ρ_c/ρ_{TF}	E_a^c	L_w ($A_y;A_o$)	Test	Bottom BC	Result
S48a	15 vs 80	0.0005/0.05	1.6	2920/2920	360	TF only [d]	-	closed	YPS
S1b	0 vs 2	0.05	1.6	3300	360	0	-	open	YPVSI
S2d	0 vs 5	0.05	1.6	3300	360	0	-	open	YPVSI
S3c	0 vs 10	0.05	1.6	3300	360	0	-	open	YPVSI
S4c	0 vs 15	0.05	1.6	3300	360	0	-	open	YPVSI
S5c	0 vs 20	0.05	1.6	3300	360	0	-	open	YPVSI
S7d	0 vs 40	0.0005/0.05	1.6	3300	360	50	-	closed	YPVSI
S7e	0 vs 40	0.05	1.6	3300	360	0	-	open	YPVSI
S8b	0 vs 50	0.05	1.6	3300	360	0	-	open	YPVSI
S9b	0 vs 60	0.0005/0.05	1.6	3300	360	50	-	closed	YPVSI
S10c	0 vs 80	0.05	1.6	3300	360	0	-	open	YPVSI
S10d	0 vs 80	0.0005/0.05	1.6	3300	360	50	-	closed	YPVSI
S14p	2 vs 5	0.0005/0.05	1.6	2920/3300	360	TF only [d]	-	closed	YPVSI
S15f	2 vs 10	0.0005/0.05	1.6	3300	360	TF only [d]	-	closed	YPVSI
S15h	2 vs 10	0.05	1.6	2920/3300	360	TF only [d]	ΔT_p =250^{o}C	open	YPVSI
S15g	2 vs 10	0.05	1.6	2920/3300	185	1100	-	closed	YPVSI
S16d	2 vs 20	0.0005/0.05	1.6	2920/3300	360	TF only [d]	-	closed	YPVSI
S17b	2 vs 40	0.05	1.6	3300	360	0	-	open	YPVSI
S17h	2 vs 40	0.0005	1.6	3300	360	" 1100;0 "	-	open	YPVSI
S17o	2 vs 40	0.0005/0.05	1.6	3300	360	50	-	closed	YPVSI
S17q	2 vs 40	0.0005/0.05	1.6	2920/3300	360	TF only [d]	-	closed	YPVSI
S17r	2 vs 40	0.0005/0.05	1.6	2920/3300	360	50	-	closed	YPVSI
S17s	2 vs 40	0.0005/0.05	1.6	3300	360	TF only [d]	-	closed	YPVSI
S18a	2 vs 80	0.05	1.6	3300	360	0	-	open	YPVSI
S18a2	2 vs 80	0.05	1.6	3300	360	0	tw=11km	open	YPVSI
S18q	2 vs 80	0.0005/0.05	1.6	3300	360	50	-	closed	YPVSI
S18s	2 vs 80	0.0005/0.05	1.6	2920/3300	360	TF only [d]	-	closed	YPVSI
S18u	2 vs 80	0.0005/0.05	1.6	3300	360	TF only [d]	-	closed	YPVSI
S19a	2 vs 100	0.05	1.6	3300	360	0	-	open	YPVSI
S21b	5 vs 10	0.0005/0.05	1.6	2920/3300	360	50	-	closed	YPVSI
S21c	5 vs 10	0.0005/0.05	1.6	3300	360	50	-	closed	YPVSI
S23c	5 vs 20	0.0005/0.05	1.6	3300	360	50	-	closed	YPVSI
S23d	5 vs 20	0.0005/0.05	1.6	2920/3300	360	50	-	closed	YPVSI
S23f	5 vs 20	0.0005/0.05	1.6	2920/3300	360	TF only [d]	-	closed	YPVSI
S26b	5 vs 40	0.0005/0.05	1.6	3300	360	50	-	closed	YPVSI
S26d	5 vs 40	0.0005/0.05	0.05	2920/3300	360	50	-	closed	YPVSI
S28a	5 vs 80	0.0005/0.05	1.6	3300	360	50	-	closed	YPVSI
S28d	5 vs 80	0.0005/0.05	1.6	2920/3300	360	TF only [d]	-	closed	YPVSI
S14n	2 vs 5	0.0005/0.05	1.6	2920/3300	360	50	-	closed	Double SI
S14q	2 vs 5	0.0005/0.01	0.8	3160/3160	360	50	-	closed	Close to OPS
S14l	2 vs 5	0.0005	1.6	3300	360	" 2.2;5 "	-	open	Close to OPS
S15c	2 vs 10	0.0005/0.05	1.6	3300	360	1100	-	closed	Close to OPS
S15i	2 vs 10	0.0005/0.01	0.8	3160/3160	360	50	-	closed	Close to OPS
S16a	2 vs 20	0.0005/0.05	1.6	3300	360	50	-	closed	Close to OPS
S17g	2 vs 40	0.0005	1.6	3300	360	" 0;1100 "	-	open	Close to OPS
S17m	2 vs 40	0.0005	1.6	2920/3300	360	TF only [d]	-	closed	Close to OPS

continued on the next page. . .

...continued

Run	A_y,A_o	γ_{TF}/γ_c	γ_m	ρ_c/ρ_{TF}	E_a^c	L_w (A_y; A_o)	Test	Bottom BC	Result
S18h	2 vs 80	0.0005	1.6	3300	360	" 0;1100 "	-	open	Close to OPS
S18m	2 vs 80	0.0005	1.6	2920/3300	360	TF only [d]	-	closed	Close to OPS
S24a	5 vs 30	0.0005	1.6	3300	360	1100	-	open	Close to OPS
S25a	5 vs 35	0.0005	1.6	3300	360	1100	-	open	Close to OPS
S25b	5 vs 35	0.0005	1.6	3300	360	1100	E_a^m =390 kJ/mol	open	Close to OPS
S25c	5 vs 35	0.0005	1.6	3300	360	1100	E_a^m =360 kJ/mol	open	Close to OPS
S25d	5 vs 35	0.0005	1.6	3300	360	1100	E_a^m =300 kJ/mol	open	Close to OPS
S26fiv	5 vs 40	0.01	1.6	3300	360	1100	SWL	open	Close to OPS
S27d	5 vs 50	0.0005	1.6	3300	360	" 20;142 "	-	open	Close to OPS
S29b	5 vs 120	0.0005	1.6	3300	360	1100	-	open	Close to OPS
S32b	7 vs 70	0.0005	1.6	3300	360	1100	E_a^m =390 kJ/mol	open	Close to OPS
S32c	7 vs 70	0.0005	1.6	3300	360	1100	E_a^m =360 kJ/mol	open	Close to OPS
S32d	7 vs 70	0.0005	1.6	3300	360	1100	E_a^m =300 kJ/mol	open	Close to OPS
S33a	7 vs 80	0.0005	1.6	3300	360	1100	-	open	Close to OPS
S33b	7 vs 80	0.0005	1.6	3300	360	1100	E_a^m =390 kJ/mol	open	Close to OPS
S33c	7 vs 80	0.0005	1.6	3300	360	1100	E_a^m =360 kJ/mol	open	Close to OPS
S33d	7 vs 80	0.0005	1.6	3300	360	1100	E_a^m =300 kJ/mol	open	Close to OPS
S34a	7 vs 90	0.0005	1.6	3300	360	1100	-	open	Close to OPS
S34c	7 vs 90	0.0005	1.6	3300	360	1100	E_a^m =390 kJ/mol	open	Close to OPS
S34d	7 vs 90	0.0005	1.6	3300	360	1100	E_a^m =360 kJ/mol	open	Close to OPS
S35b	7 vs 120	0.0005	1.6	3300	360	1100	-	open	Close to OPS
S37d	10 vs 40	0.0005	0.1	3300	360	1100	-	open	Close to OPS
S37e	10 vs 40	0.0005	0.075	3300	360	1100	-	open	Close to OPS
S37h	10 vs 40	0.0005	0.05	3300	360	" 0;1100 "	-	open	Close to OPS
S43a	10 vs 140	0.0005	1.6	3300	360	1100	-	open	Close to OPS
S44a	10 vs 150	0.0005	1.6	3300	360	1100	-	open	Close to OPS
S46a	15 vs 40	0.0005	0.05	3300	360	1100	-	open	Close to OPS
S50b	20 vs 60	0.0005	0.05	3300	360	1100	-	open	Close to OPS
S51b	20 vs 80	0.0005	0.1	3300	360	1100	-	open	Close to OPS
S51c	20 vs 80	0.0005	0.08	3300	360	1100	-	open	Close to OPS
S56a	25 vs 80	0.0005	0.05	3300	360	1100	-	open	Close to OPS
S57b	25 vs 100	0.0005	0.075	3300	360	1100	-	open	Close to OPS
S49h	20 vs 40	0.0005	0.005	3300	360	1100	-	open	OPS-mode 1, SB, YPD
S49i	20 vs 40	0.0005	0.005	3300	360	" 151;238 "	-	open	OPS-mode 1, SB, YPD
S49j	20 vs 40	0.0005	0.005	3300	360	" 76;119 "	-	open	OPS-mode 1, SB, YPD
S34b	7 vs 90	0.0005	0.1	3300	360	1100	-	open	OPS-mode 1, SB
S53a	20 vs 130	0.0005	0.1	3300	360	1100	-	open	OPS-mode 1, SB
S14c	2 vs 5	0.0005	1.6	3300	360	1100	-	open	OPS-mode 2, SB
S14d	2 vs 5	0.0005	1.6	3300	360	1100	tw=11km	open	OPS-mode 2, SB
S14e	2 vs 5	0.05	1.6	3300	185	0	-	open	OPS-mode 2, SB
S22j	5 vs 15	0.0005	0.1	3300	360	1100	-	open	OPS-mode 2, SB
S22k	5 vs 15	0.0005	0.05	3300	360	1100	-	open	OPS-mode 2, SB
S3a	0 vs 10	0.0005	1.6	3300	360	1100	-	open	OPS-mode 1
S3b	0 vs 10	0.0005	0.05	3300	360	1100	-	open	OPS-mode 1
S4a	0 vs 15	0.0005	1.6	3300	360	1100	-	open	OPS-mode 1

continued on the next page...

. . . continued

Run	A_y,A_o	γ_{TF}/γ_c	γ_m	ρ_c/ρ_{TF}	E_a^c	L_w $(A_y;A_o)$	Test	Bottom BC	Result
S4b	0 vs 15	0.0005	0.05	3300	360	1100	-	open	OPS-mode 1
S5a	0 vs 20	0.0005	1.6	3300	360	1100	-	open	OPS-mode 1
S6a	0 vs 30	0.0005	1.6	3300	360	1100	-	open	OPS-mode 1
S7a	0 vs 40	0.0005	1.6	3300	360	1100	-	open	OPS-mode 1
S7b	0 vs 40	0.0005	0.05	3300	360	1100	-	open	OPS-mode 1
S8a	0 vs 50	0.0005	1.6	3300	360	1100	-	open	OPS-mode 1
S9a	0 vs 60	0.0005	1.6	3300	360	1100	-	open	OPS-mode 1
S10a	0 vs 80	0.0005	1.6	3300	360	1100	-	open	OPS-mode 1
S11a	0 vs 100	0.0005	1.6	3300	360	1100	-	open	OPS-mode 1
S12b	0 vs 120	0.0005	1.6	3300	360	1100	-	closed	OPS-mode 1
S21a	5 vs 10	0.0005	0.1	3300	360	1100	-	open	OPS-mode 1
S26a	5 vs 40	0.0005	1.6	3300	360	1100	-	open	OPS-mode 1
S26ai	5 vs 40	0.0001	1.6	3300	360	1100	-	open	OPS-mode 1
S26f	5 vs 40	0.0005	1.6	3300	360	1100	SWL	open	OPS-mode 1
S26fi	5 vs 40	0.0001	1.6	3300	360	1100	SWL	open	OPS-mode 1
S26fii	5 vs 40	0.005	1.6	3300	360	1100	SWL	open	OPS-mode 1
S26fiii	5 vs 40	0.001	1.6	3300	360	1100	SWL	open	OPS-mode 1
S27a	5 vs 50	0.0005	1.6	3300	360	1100	-	open	OPS-mode 1
S27c	5 vs 50	0.0005	1.6	3300	360	" 42;260 "	-	open	OPS-mode 1
S29a	5 vs 100	0.0005	1.6	3300	360	1100	-	open	OPS-mode 1
S31a	7 vs 30	0.0005	0.1	3300	360	1100	-	open	OPS-mode 1
S34e	7 vs 90	0.0005	1.6	3300	360	1100	E_a^m =300 kJ/mol	open	OPS-mode 1
S35a	7 vs 100	0.0005	1.6	3300	360	1100	-	open	OPS-mode 1
S37f	10 vs 40	0.0005	0.05	3300	360	1100	-	open	OPS-mode 1
S38a	10 vs 50	0.0005	0.1	3300	360	1100	-	open	OPS-mode 1
S39b	10 vs 60	0.0005	0.1	3300	360	1100	-	open	OPS-mode 1
S47a	15 vs 60	0.0005	0.1	3300	360	1100	-	open	OPS-mode 1
S47b	15 vs 60	0.0005	0.08	3300	360	1100	-	open	OPS-mode 1
S47c	15 vs 60	0.0005	0.06	3300	360	1100	-	open	OPS-mode 1
S47d	15 vs 60	0.0005	0.05	3300	360	1100	-	open	OPS-mode 1
S49k	20 vs 40	0.0005	0.005	3300	360	" 38;60 "	-	open	OPS-mode 1
S49l	20 vs 40	0.0005	0.005	3300	360	" 19;30 "	-	open	OPS-mode 1
S51d	20 vs 80	0.0005	0.06	3300	360	1100	-	open	OPS-mode 1
S51e	20 vs 80	0.0005	0.05	3300	360	1100	-	open	OPS-mode 1
S52b	20 vs 100	0.0005	0.1	3300	360	1100	-	open	OPS-mode 1
S57a	25 vs 100	0.0005	0.05	3300	360	1100	-	open	OPS-mode 1
S1a	0 vs 2	0.0005	1.6	3300	360	1100	-	open	OPS-mode 2
S2a	0 vs 5	0.0005	1.6	3300	360	1100	-	open	OPS-mode 2
S2b	0 vs 5	0.0005	0.05	3300	360	1100	-	open	OPS-mode 2
S2c	0 vs 5	0.0005/0.05	1.6	3300	360	50	-	closed	OPS-mode 2
S5b	0 vs 20	0.0005/0.05	1.6	3300	360	50	-	closed	OPS-mode 2
S14i	2 vs 5	0.0005	1.6	3300	360	" 17;42 "	-	open	OPS-mode 2
S14j	2 vs 5	0.0005	1.6	3300	360	" 8.5;20 "	-	open	OPS-mode 2
S14k	2 vs 5	0.0005	1.6	3300	360	" 4.3;10 "	-	open	OPS-mode 2
S14m	2 vs 5	0.0005/0.05	1.6	3300	360	50	-	closed	OPS-mode 2
S14r	2 vs 5	0.0005/0.01	0.8	3160/3300	360	50	-	closed	OPS-mode 2
S14s	2 vs 5	0.05/0.0005	1.6	3300	360	TF only [d]	-	closed	OPS-mode 2
S15b	2 vs 10	0.0005	1.6	3300	360	1100	-	open	OPS-mode 2

continued on the next page. . .

. . . continued

Run	A_y,A_o	γ_{TF}/γ_c	γ_m	ρ_c/ρ_{TF}	E_a^c	L_w (A_y; A_o)	Test	Bottom BC	Result
S15j	2 vs 10	0.0005/0.01	0.8	3160/3300	360	50	-	closed	OPS-mode 2
S16f	2 vs 20	0.0005/0.01	0.6	3160/3160	360	50	-	closed	OPS-mode 2
S16g	2 vs 20	0.0005/0.01	0.8	3160/3160	360	50	-	closed	OPS-mode 2
S17c	2 vs 40	0.0005	1.6	3300	360	1100	-	open	OPS-mode 2
S17e	2 vs 40	0.0005	1.6	3300	360	1100	-	open	OPS-mode 2
S17n	2 vs 40	0.0005	1.6	3300	360	TF only [d]	-	closed	OPS-mode 2
S17t	2 vs 40	0.0005/0.01	0.6	3160/3160	360	50	-	closed	OPS-mode 2
S17v	2 vs 40	0.0005/0.01	0.8	3160/3160	360	50	-	closed	OPS-mode 2
S18b	2 vs 80	0.0005	1.6	3300	360	1100	-	open	OPS-mode 2
S18b2	2 vs 80	0.0005	1.6	3300	360	1100	tw=11km	open	OPS-mode 2
S18b3	2 vs 80	0.0005	1.6	3300	360	1100	tw=30 km	open	OPS-mode 2
S18b4	2 vs 80	0.0005	1.6	3300	360	1100	tw=50 km	open	OPS-mode 2
S18b5	2 vs 80	0.0005	1.6	3300	360	1100	tw=70 km	open	OPS-mode 2
S18d	2 vs 80	0.0007	1.6	3300	360	1100	-	open	OPS-mode 2
S18e	2 vs 80	0.001	1.6	3300	360	1100	-	open	OPS-mode 2
S18p	2 vs 80	0.0005	0.6	2920/3300	360	TF only [d]	-	closed	OPS-mode 2
S19b	2 vs 100	0.0005	1.6	3300	360	1100	-	open	OPS-mode 2
S20a	2 vs 120	0.0005	1.6	3300	360	1100	-	open	OPS-mode 2

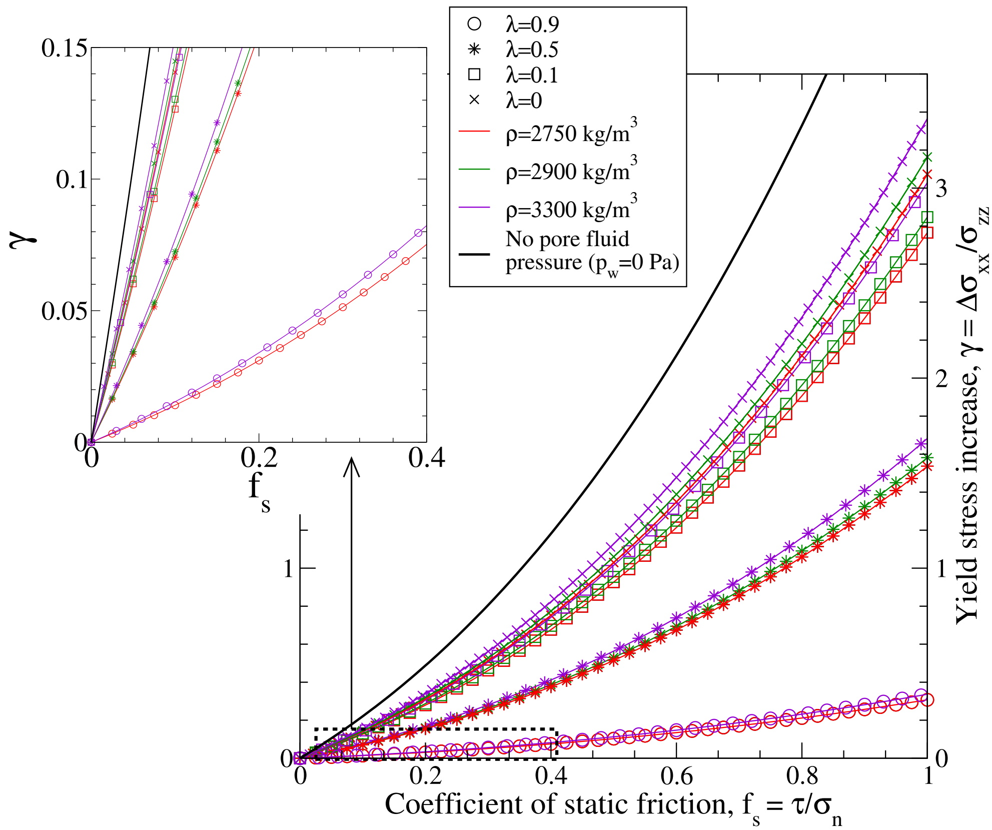

Figure S1. Brittle parameter (yield strength increase with depth), γ, used in eq. 1 to compute brittle stresses. The brittle parameter is a function of rock friction coefficient f_s, rock and water densities, ρ and ρ_w and pore fluid pressure coefficient, λ, according to eq. 4 and 5 in the main text from Turcotte and Schubert (1982). The inserted graph is a close-up on f_s values <0.4.

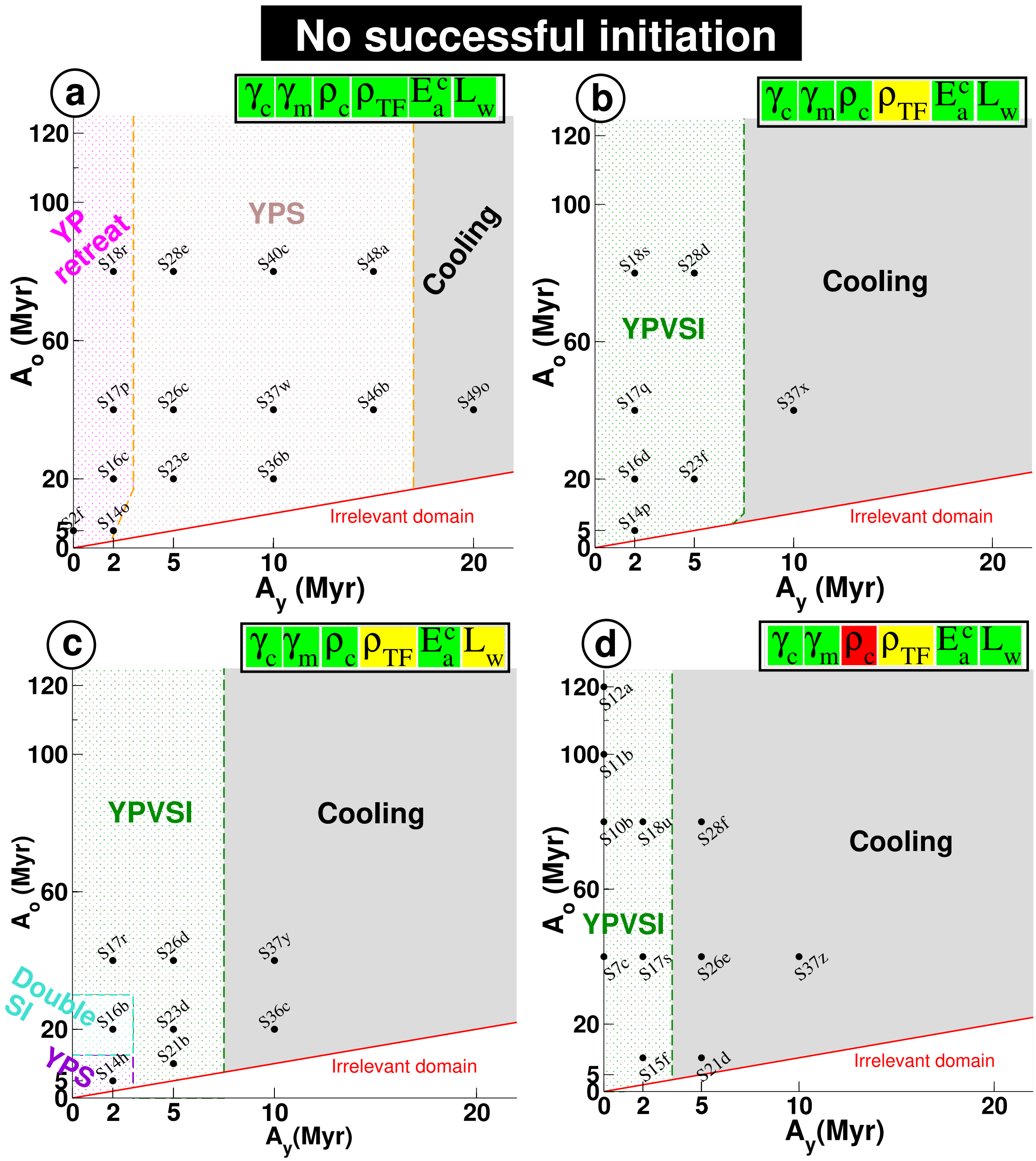

Figure S2. Regime diagrams as a function of the mechanical property combination failing in achieving OPS, showing the experiments used to defined the boundaries between different regimes. The box colors correspond to parameter ranges shown in Fig. 3. The acronym meanings are defined in Table S1 caption. The parameter combination γ_c, γ_m, ρ_c, ρ_{TF}, and L_w, is, respectively, in panel (a): 0.05, 1.6, 2920 kg.m^{-3}, 2920 kg.m^{-3}, and 0 km; in panel (b) 0.05, 1.6, 2920 kg.m^{-3}, 3300 kg.m^{-3}, and 0 km; in panel (c): 0.05, 1.6, 2920 kg.m^{-3}, 3300 kg.m^{-3}, and 50 km; in panel (d): 0.05, 1.6, 3300 kg.m^{-3}, 3300 kg.m^{-3}, and 0 km; In all panels, E_a^c =360 kJ/mol.

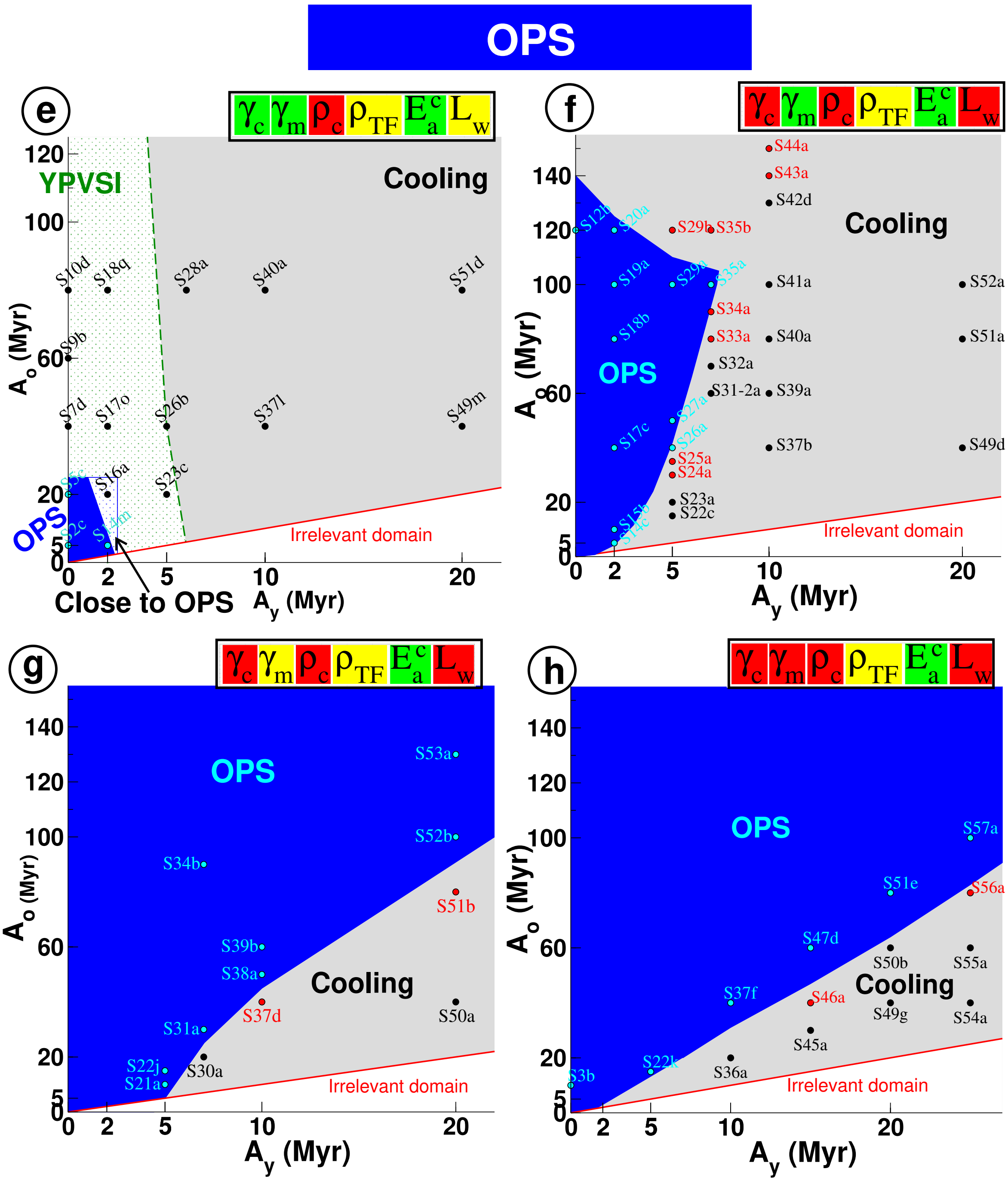

Figure S3. Regime diagrams as a function of the mechanical property combination succeeding in achieving OPS, showing the experiments used to defined the boundaries between different regimes. The box colors correspond to parameter ranges shown in Fig. 3. Panels are labeled to respect the labeling used in Fig. 6. The experiments shown in black, red and light blue, respectively, refer to cases of cooling, close to OPS and OPS, respectively. The parameter combination γ_c, γ_m, ρ_c, ρ_{TF}, and L_w, is, respectively, in panel (e): 0.05, 1.6, 3300 kg.m^{-3}, 3300 kg.m^{-3}, and 50 km; in panel (f): 5$\times$10^{-4}, 1.6, 3300 kg.m^{-3}, 3300 kg.m^{-3}, and 1100 km; in panel (g): 5$\times$10^{-4}, 0.1, 3300 kg.m^{-3}, 3300 kg.m^{-3}, and 1100 km; and in panel (h): 5$\times$10^{-4}, 0.05, 3300 kg.m^{-3}, 3300 kg.m^{-3}, and 1100 km. In all panels, E_a^c =360 kJ/mol.

S2 Minimum extent of crust weakening allowing OPS as a function of rheology

We seek for the minimum distance from the TF over which the crust must be weakened (L_w) to allow OPS, in order to compare it to the damage/alteration extent around a TF in nature. As mentioned in the main text, OPS triggering basically depends on plate bending ability, that we assume to depend on the lateral extent of weakened crust. To test it, we first estimate the bending length as a function of the plate age, for the rheological set leading to self-sustained OP subduction (Fig. 6f). Experiments are performed by varying the age A_o of the plate imposed on the left-hand side of the TF while on the other side the asthenosphere is modelled right below the crust base (Fig. S4a). An horizontal profile of velocity computed at mid-depth within the OP is used to estimate the plate bending length (Fig. S4a, top panel): L_0 corresponds to the distance between the infant slab extremity (high velocities) and the location backwards where velocities vanish to zero. The obtained bending length, L_0, roughly increases as the square root of A_0, meaning that L_0 and plate thickness are at first order proportional (Fig. S4b).
We next study OPS triggering as a function of the crust "damage" extent for a set of plate age pairs showing OPS when the whole oceanic crust is weakened (L_w =1100 km). These age pairs are selected in order to cover a wide range of YP age (2 to 20 Myr). The area of weakened crust, L_w, is reduced from 1110 km to the respective plate bending length L_0 of each plate, and even lowered down to a fraction of L_0 (1/2, 1/4, and 1/8). For a very thin YP (A_y =2 Myr), OPS is observed without mantle weakening (γ_m=1.6) and the minimum L_w allowing OPS is short ($L_w = L_0/4$ =4 km and 10 km for the plate age pair 2 vs 5, Fig. S5). When the YP is 5 Myr old, the minimum L_w is L_0, already outside a realistic range ($L_0 =$ 41 km and 274 km for 5 vs 50). For a thicker YP, the mantle strength must be significantly lowered to enable OPS, as mentioned in Sect. 2.8.4. For a 10 Myr old YP and γ_m lowered to 0.05, OPS does not occur unless the crust recovers the whole box surface (L_w =1100 km, 10 vs 40). Still, when $A_y =$ 20 Myr, since OPS is not allowed if the mantle is not extremely weakened (γ_m reduced to 0.005), OPS triggering does not strongly depends on the extent of weakened crust and is observed as soon as $L_w \geq L_0/8$, that is for weakened domains shorter than 30 km.
We conclude that the domain of weakened crust to impose in the vicinity of the TF to achieve OPS is too large to be realistic, at least for classical mantle rheology, the only exception being a very thin YP (A_y =2 Myr). These results reinforce the strong resistant character of thick YP on OPS triggering.

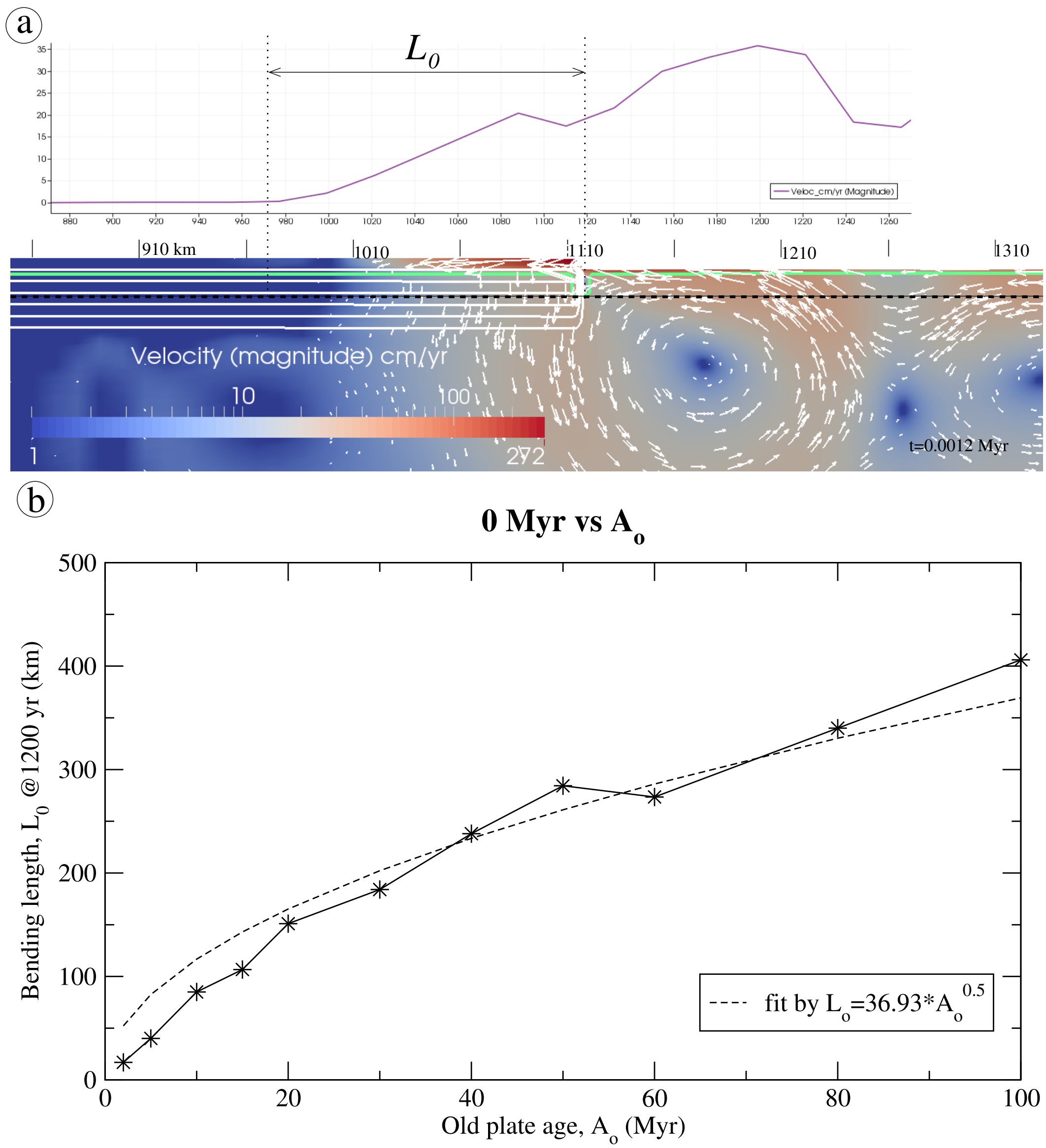

Figure S4. Estimate of the bending length, L_0, as of function of plate age, A_o, when the A_o old plate is facing a layer of asthenosphere at the TF. The set of rheological parameters is the same as used in Fig. 6f: $\gamma_c = 5 \times 10^{-4}$, γ_m =1.6, ρ_c =3300 kg.m^{-3}, ρ_{TF} =3300 kg.m^{-3}, E_a^c =360 kJ/mol, and L_w =1100 km. (a) Example of L_0 measurement in simulation S5a (A_o =20 Myr). Bottom row: Snapshot of the velocity field soon after simulation start (t =1200 yr). Isotherms (white lines) are displayed every 200^{o}C. The green thick line outlines the weak layer. Note that the velocity scale is logarithmic. Horizontal distances are measured from the box left-hand side (no vertical exaggeration). The black dotted line is the horizontal profile at mid-depth within the OP along which velocities are sampled to estimate the plate bending length L_0 (top row panel). (b) Plate bending length L_0 as a function of plate age, A_0, obtained in experiments S1a, S2a, S3a, S4a, S5a, S6a, S7a, S8a, S9a, S10a, and S11a (stars and solid line).

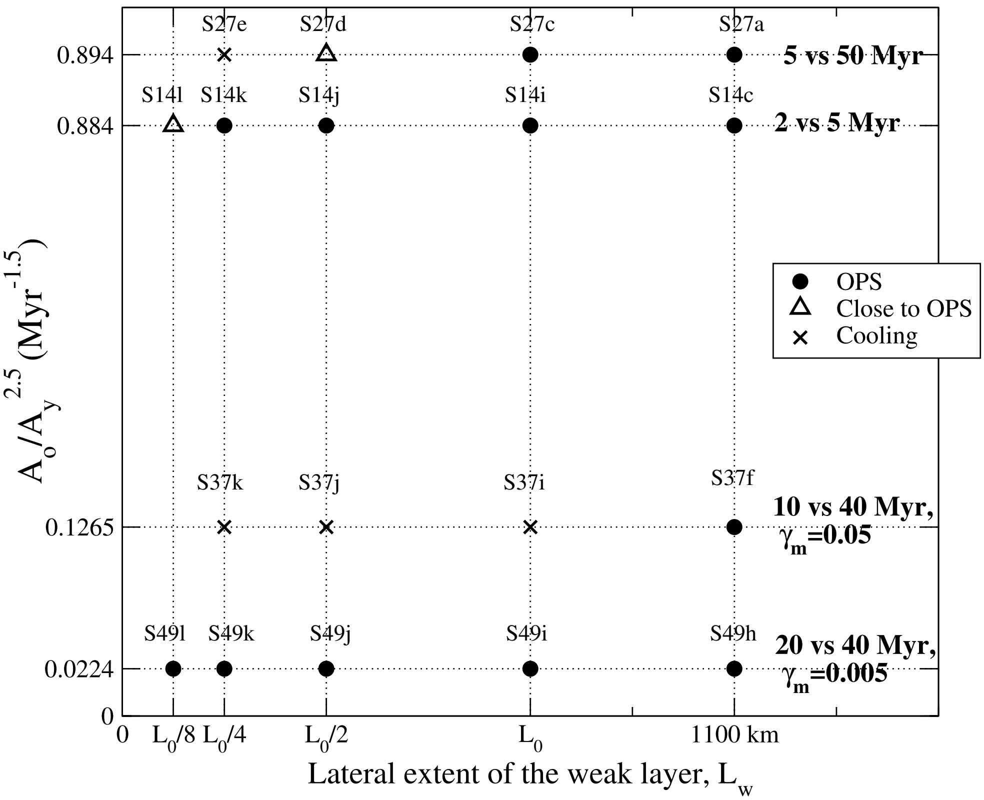

Figure S5. Regime diagram as a function of the crust weakening width, imposed away from the TF, L_w, for 4 plate age pairs and different mantle brittle parameter. L_o refers to the bending length displayed in Fig. S4b corresponding to the plate age A_o. The different plate age pairs (A_y,A_o) are depicted by a single parameter, $A_o/A_y^{2.5}$, that can be used to predict OPS occurrence for a normal mantle brittle parameter (γ_m =1.6) and for an oceanic crust assumed to be weakenened over the whole plate surface (Fig. 6f). Note that the $y-$axis is not scaled.

S3 Additional tests on OPS conditions: TF gouge strength and width; TF vs fracture zones; asthenosphere viscosity and free surface

We sum up in this section extra experiments performed to precise the mechanisms involved in OPS triggering.

We first test the necessity of the fault softness to simulate OPS, by inverting the oceanic crust and TF respective brittle strength (γ_{TF} =0.05 instead of 0.0005, while γ_c is set to 0.0005). For the plate age pairs 2 vs 5 and 2 vs 40, OPS is either prevented or postponed to the end of a first YP sinking stage when the TF gouge brittle coefficient is not drastically reduced (sim. S14s and S17u). The TF strength is thus critical to model OPS. We next wonder if OPS could be triggered by widening the fault gouge from the surface to the bottom of the fault (domain 1 in Fig. 2), by setting the fault width to 20 km instead of 8.3 km, for 2 plate age pairs: (A_y, A_o) =5 vs 15 (simulation S22t, $\gamma_c = 5 \times 10^{-5}$) and (A_y, A_o) =10 vs 40 (simulations S37r, with $\gamma_c = 5 \times 10^{-4}$ and S37s, $\gamma_c = 5 \times 10^{-5}$). Simulations show that OPS does not occur, even if the mechanical decoupling is maximized. The mechanical interplate decoupling is hence not sufficient to trigger OPS alone.
Subsequently, we investigate the possible role of the TF thermal structure. We assume that the interplate domain is very thin, since it is modeled by a stair-step (Sect. 2.2). In nature this set-up would correspond to an active transform fault. If the fault is instead inactive, the thermal state at the plate boundary is likely to be cooled by thermal conduction, and consequently possibly stronger and more resistant to plate decoupling. Besides, the fault thermal structure may depend on the distance between the spreading ridge and the location where the TF cross section is considered (Behn et al., 2007). We test the influence of the thermal structure of the TF for the plate age pair 2 vs 80 for which OPS is simulated if the crust brittle parameter γ_c is 0.0005. While for the stair-step case the width of the transition between the 2 plates is close to zero (simulation S18b), we widen the TF thermal transition to 11 km (sim. S18b2), 30 km (S18b3), 50 km (S18b4), and 70 km (S18b5), keeping the weak material forming the fault gouge at the center of the thermal transition in all cases. In the same way, the thermal transition width is enlarged to 11 km for 2 vs 5 in simulation S14d (0 km in S14c). All these experiments show OPS. We here verify that the fault gouge weakening, governed by the weak material brittle properties, is independent of temperature, and at first order independent of the fault activity in our 2D set-up. Similarly, the YP vertical sinking occurs for a stair-step transition (simulation S18a) as well as if the thermal transition width is set to 11 km (sim. S18a2).
We then test if a decrease in asthenosphere strength could help OPS triggering, as the asthenosphere viscosity should resist plate sinking. For one plate age pair yielding cooling only, even if the crust brittle parameter is significantly decreased (5 vs 15, simulation S22h), the reference asthenospheric viscosity is decreased by a factor 5, while for 2 other plate age pairs (10 vs 40, S37b2 and 20 vs 40, S49f), a factor 10 is applied. Experiments show that asthenospheric velocities and OP deformation are slightly amplified but still not enough for OPS to be triggered.

At last, the influence of the mechanical boundary condition at the box top is investigated. A free-slip condition inhibiting any vertical motion is prescribed in all the simutations presented before, whereas it has been shown that a free surface condition allowing for vertical deflection at the plate surface could strongly promote subduction initiation (Crameri et al., 2012b; Crameri and Tackley, 2016). We test how the implementation of a sticky air layer enabling for the free plate surface deformation could modify the OPS triggering modeled in our study by comparing the critical crustal brittle parameter that must be imposed to achieve OPS, with and without a free surface. Simulation S26a (Table S1) is chosen, since the plate age pair 5 vs 40 is just right above the threshold necessary for OPS triggering when the mechanical parameter set is the one displayed in Fig. 6-5 for ($\gamma_c = 0.0005$). We first perform 3 additional experiments to accurately estimate the threshold in crustal brittle parameter without free surface, $\gamma_c^{free\ slip}$ (Simulations S26ai, S26aii and S26aiii, Table S1) and find that $\gamma_c^{free\ slip} \sim 0.0025$ ($0.0001 \leq \gamma_c^{free\ slip} < 0.005$).
Next, new experiments are run in which a thin low viscosity layer is inserted at the surface of the simulation box, 5 km thick (Fig. S6). This low viscosity layer is assumed to be made of water (density of 1000 kg.m^{-3}) as the transform faults considered in this study are all oceanic. Therefore, this low viscosity layer is dubbed a "sticky water layer" (SWL). The rheological parameters of the SWL are tuned to minimize its viscosity ($E_a = 0$ kJ/mol, $\gamma_{SWL} = 5 \times 10^{-4}$ for instance) so that $\nu_{SWL} \sim 3.8 \times 10^{11}$ Pa.s. Crameri et al. (2012a) have shown that, to correctly reproduce a true surface boundary condition, the SWL properties must enable to verify: $C_{Stokes} \ll 1$, where C_{Stokes} is the ratio between the pressure difference at the box sur-

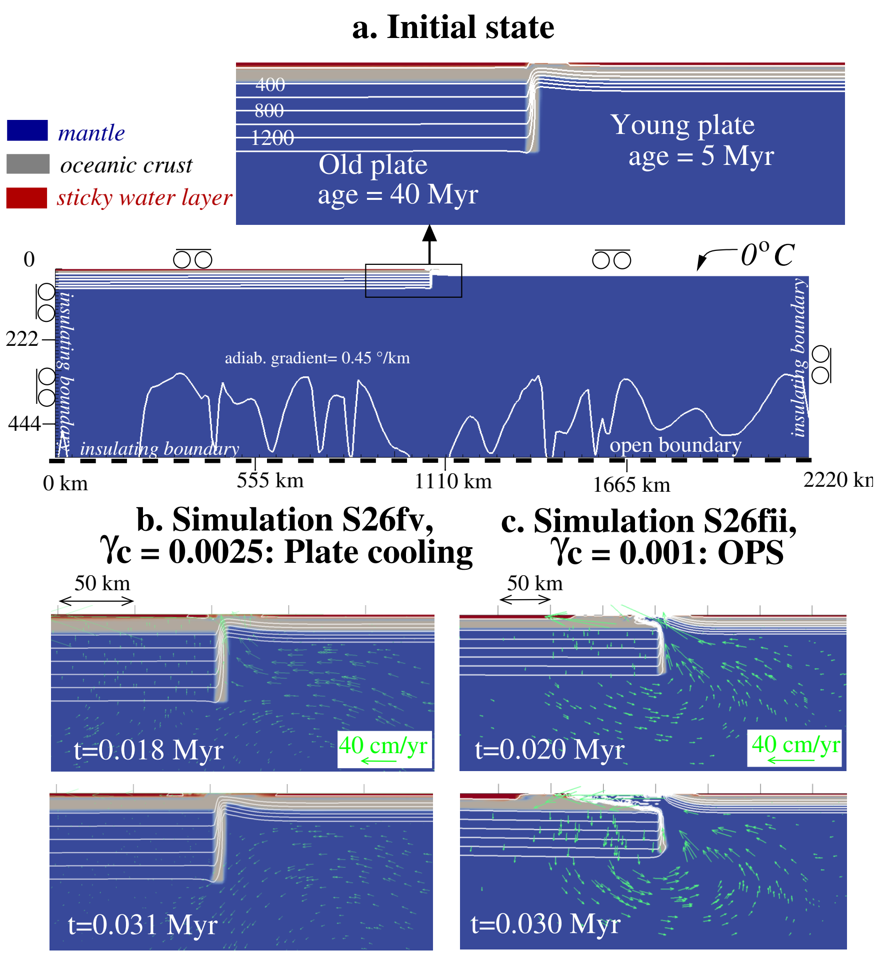

Figure S6. Experiments performed with a sticky water layer. (a) Boundary conditions at the start of the simulations including a weak oceanic crust ($\gamma_c \leq$0.05). (b) Experiment S26fv ($\gamma_c = 0.025$, Table S1): close-up on the plate boundary. (c) Experiment S26fiii ($\gamma_c = 0.001$).

-face and the vertical stress resulting in the surface deflection. For a Stokes flow, C_{Stokes} writes as (Crameri et al., 2012a):

$$C_{Stokes} = \frac{1}{16}\frac{\Delta\rho}{\rho_m^{ref}}\left(\frac{H_0}{H_{SWL}}\right)^3 \frac{\nu_{SWL}}{\nu_{mantle}} \tag{1}$$

where $\Delta\rho$ is the slab density contrat ($= \alpha\rho_m^{ref}\Delta T \sim 150\,\mathrm{kg.m}^{-3}$), H_0 is the simulation box height (Table 2), H_{SWL} is the SWL thickness, ν_{SWL} is the SWL viscosity and ν_{mantle} is the mantle viscosity. By recalling that $\nu_{mantle} = \nu_{asth} = 2.74 \times 10^{19}$ Pa.s (caption of Table S1), the SWL viscosity allows for verifying the required condition ($C_{Stokes} \sim 5.39 \times 10^{-5}$).
A short preliminary run is performed with the reference brittle parameter of the oceanic crust ($\gamma_c = 0.05$) during $\sim$ 20 kyr to let the transform fault topography equilibrate (Fig. S6a). The crust brittle parameter is then varied between 0.0005 and 0.05 (Simulations S26f to S26fvi, Table S1). We find that $\gamma_c^{free\ surface} \sim 0.0175$ ($0.01 \leq \gamma_c^{free\ surface} < 0.025$, Fig. S6b and c). The threshold in γ_c allowing for OPS is thus decreased by a factor $\sim$ 7 when the free surface is simulated for the plate age pair 5 vs 40.

S4 Modes of OPS

In Sect. 3.1 we analyse the velocity fields simulated during modes 1 and 2 (Fig. S7) and show that these modes of OPS initiation are associated with a particular YP kinematics. Mode 1 is related to a roughly motionless YP remains while asthenospheric velocities are high ($\geq$ 20 cm/yr, Fig. S7) and focused at the TF towards the OP surface. Furthermore, velocities are not homogeneous along the YP but slighly increase towards the TF. On the contrary, in mode 2 the velocity field across the YP is homogeneous but also roughly constant from the YP base to the asthenosphere where speeds are high (between 25 and 100 cm/yr). Moreover, within the set of simulations showing OPS (Sect. 3.2), we find that mode 2 occurs when $A_y \leq$2 Myr, for various rheological sets, or if $A_y =$5 Myr, provided that the mantle brittle parameter is reduced. In all these experiments, the viscosity ratio between the lithospheric mantle strength at the Moho and the asthenospheric viscosity (10^{18} Pa.s in most experiments) is $\lesssim 10^2$ to 10^3 (Fig. S8). Hence the strength of the YP bottom part is the closest to the asthenospheric one in mode 2. On the contrary, the focusing of asthenosphere flows at the TF in mode 1 is observed when the viscosity offset between the YP mantle and the underlying mantle exceeds 10^3. We conclude that mode 2 takes place by a stronger coupling between the YP and the asthenosphere. Still, as slab roll-back during OPS is all the faster than the OP is aged, the crust transfer in mode 2 from the YP towards the OP gets hampered at some point for thick OPs. A switch from mode 2 to mode 1 is then observed in some experiments (S16f; S17c,n; and S18p, Table S1).
Similarly, several simulations performed with $A_y =$0 Myr show an OPS initiation following an intermediate mode: the kinematic coupling YP/asthenosphere is less clear, and velocities are not laterally transferred far away from to TF. To understand this result, one may notice that in this particular case the 1200^{o}C isotherm (considered as the lithospheric base) is located at 5 km depth, i.e., shallower than the modelled Moho (8.3 km). The YP plate for $A_y =$0 Myr is thus mainly a "crustal plate" devoid of a mantle base, and, depending on the strain-rate, more or less significantly weaker than the asthenosphere (Fig. S8). The mechanical coupling between the YP and the hot mantle is high in simulations S1a to S2b (considered as mode 2 OPS), but is not continuously strong through time in simulations S3a to S11a (Table S1). To simplify these later experiments performed with $A_y =$0 Myr are considered as mode 1 OPS .

S5 Amount of lithospheric mantle weakening to achieve OPS

Our study shows that OPS is enhanced if the lithospheric mantle is weak. The reduction in mantle strength depends on the plate age pair and on other mechanical parameters, such as γ_m. A first-order estimate of the lithospheric mantle softening necessary to model OPS is derived by computing the ratio of the maximum lithospheric viscosity along a vertical profile located 50 km away from the TF at the start of simulation, for experiments that do not show OPS over the viscosity at the same depth for experiments achieving OPS (for the closest parameterization setting). For instance, by comparing simulations S14t and S14c (2 vs 5, Table S1), this strength ratio is $\sim$1.4 in the OP, observed at the Moho depth; between S51a and S51d (20 vs 80), it is obtained in the mantle layer (27 km depth) of the OP and is equal to $\sim$28; between S34a and S34e (7 vs 90), the ratio of maximum viscosity is observed at 15 km depth in the OP, equal to 35; and between S49d and S49h (20 vs 40), it is observed in the OP mantle (at 20 km depth) and reaches $\sim$280. The mantle weakening enabling OPS is thus low to moderate for young plates and high plate age offsets, and larger when the plate age contrast is small.
In our experiments, the maximum strength in the mantle lithosphere described above always corresponds to deviatoric stresses encompassed between 19 and 35 MPa, except in the 7 vs 90 case for which the stress at 15 km depth reaches $\sim$190 MPa in Simulation S34a (no OPS) and $\sim$1030 MPa in Sim. S34e (OPS).
Are such mantle strength decreases realistic? One may discuss different mechanisms of mantle weakening in oceanic lithosphere, such as (1) low-temperature plasticity (so-called Peierls'creep, Goetze and Evans, 1979), that promotes the deformation of slab and plate base (Garel et al., 2014), (2) creep by grain-boundary sliding (GBS, Drury, 2005), (3) grain-size reduction when diffusion linear creep is activated (e.g., Montési and Hirth, 2003), or (4) fluid-related weakening. Demouchy et al. (2013) have shown that mantle strength can significantly be lowered by Peierls'plasticity in the $\sim$700-1000^{o}C range, but stresses remains >500 MPa for a reference strain rate of 10^{-14} s^{-1}. GBS or grain-size sensitive-power law regime (2) is not experimentally well constrained. According to Drury (2005), GBS creep operates if stresses are >100 MPa, for large strain and low temperature (<800^{o}C).

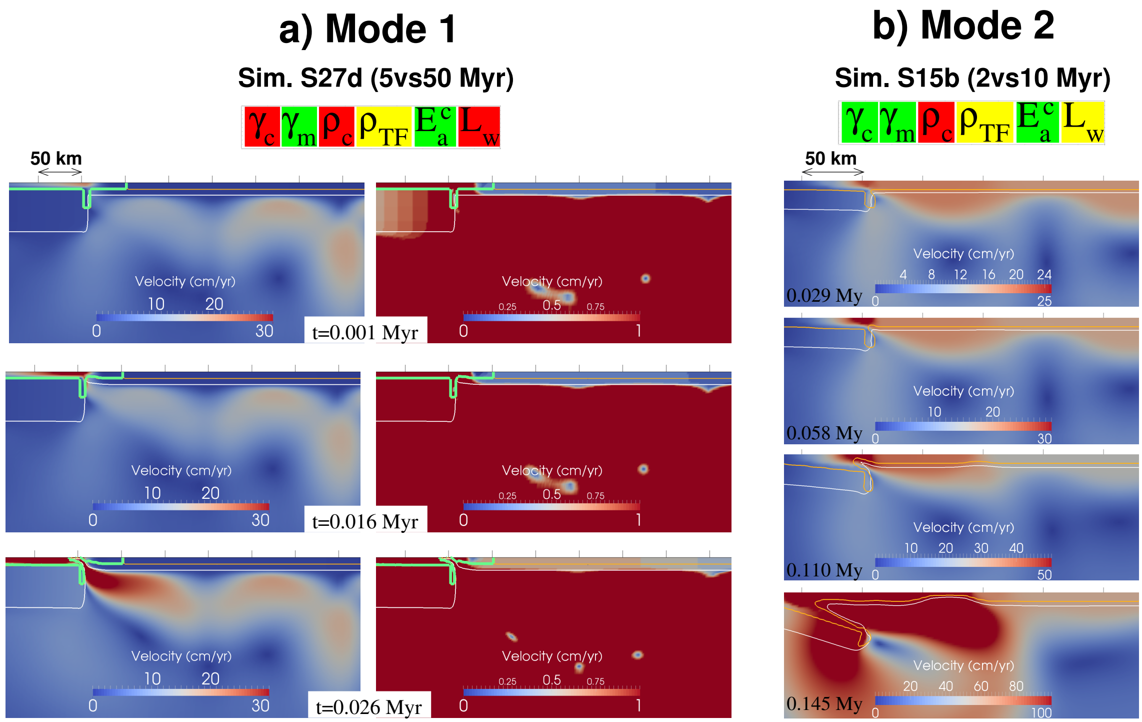

Figure S7. Velocity field obtained (a) in Simulation S27d illustrating mode 1 OPS and (b) Simulation S15b illustrating mode 2 OPS. White line: 1200^{o}C isotherm. Yellow line: boundary between the mantle and the oceanic crust. Green thick outline: limit of the weak material. Note that in panel a, the velocity color scale is saturated to 1 cm/yr in the right-hand column to highlight low speeds within the younger plate. No vertical exaggeration.

As a consequence, we assume that if Peierls'plasticity or ductile creep by grain-boundary sliding were implemented in our numerical model, they would not be activated in most of our experiments, except in the case of Simulation S34a in which they might limit the brittle strength and eventually favor OPS. Note however that the plate age pair in Sim. S34a, 7 vs 90, does not correspond to any of the 3 potential candidates of subduction initiation found in nature likely to have matched the conditions of spontaneous subduction (IBM, Yap, and Mattew & Hunter, Fig. 6e-h). Weakening processes (3) and (4) are discussed in the main text (section 5.1.4).

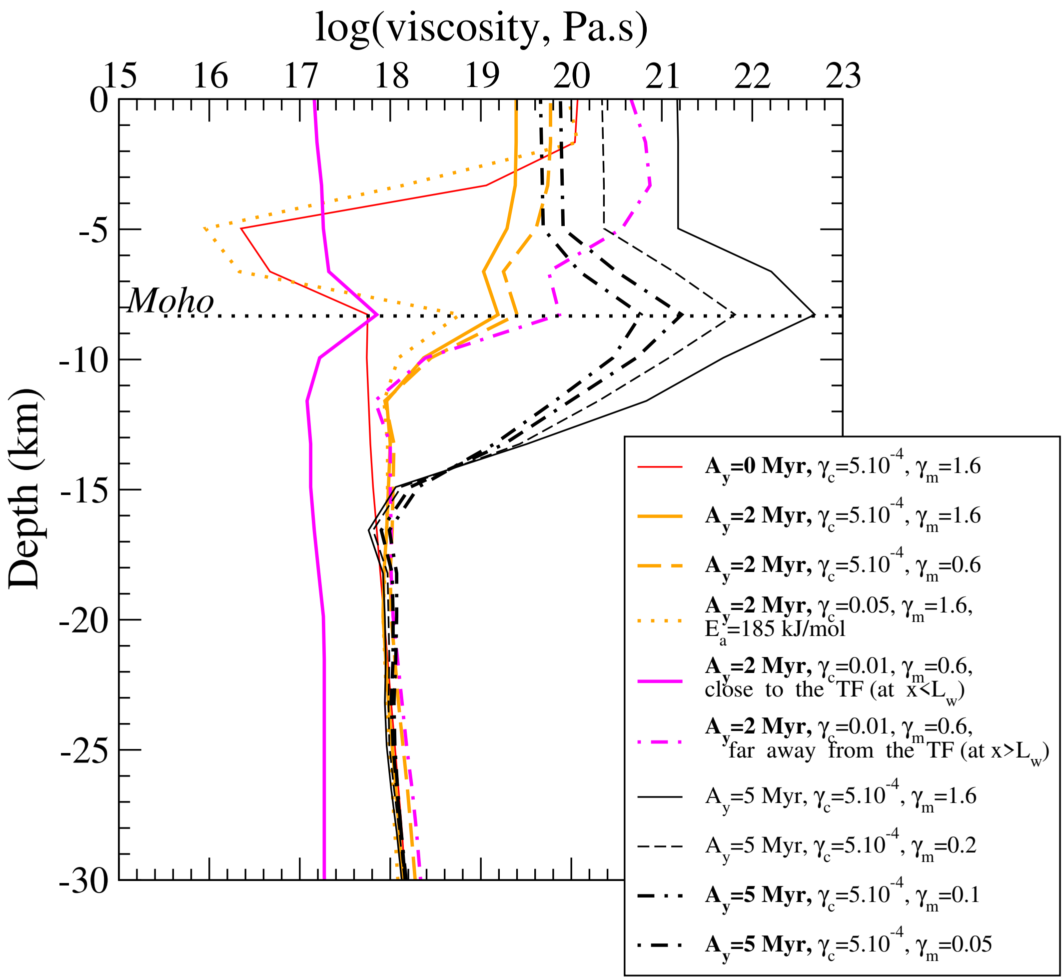

Figure S8. Viscosity profiles at simulation start as a function of plate age and rheological set. When not mentioned, profiles are computed at the center of the plate (555 km away from the closer vertical box boundary). The asthenospheric viscosity is 10^{18} Pa.s in most experiments, but may vary as viscosity is strain rate-dependent in our model. Thick lines and bold polices are used for viscosity profiles corresponding to a mode 2 initiation where the considered plate is the YP.

References

Behn, M., Boettcher, M., and Hirth, G. (2007). Thermal structure of oceanic transform faults. *Geology*, **4**, 307–310. 10.1130/G23112A.1.

Crameri, F. and Tackley, P. J. (2016). Subduction initiation from a stagnant lid and global overturn: new insights from numerical models with a free surface. *Progress in Earth and Planetary Science*, **3**(1), 30.

Crameri, F., Schmeling, H., Golabek, G., Duretz, T., Orendt, R., Buiter, S., May, D., Kaus, B., Gerya, T., and Tackley, P. (2012a). A comparison of numerical surface topography calculations in geodynamic modelling: an evaluation of the 'sticky air'method. *Geophysical Journal International*, **189**(1), 38–54.

Crameri, F., Tackley, P., Meilick, I., Gerya, T., and Kaus, B. (2012b). A free plate surface and weak oceanic crust produce single-sided subduction on Earth. *Geophys. Res. Lett.*, **39**. 10.1029/2011GL050046.

Demouchy, S., Tommasi, A., Ballaran, T. B., and Cordier, P.: Low strength of Earth's uppermost mantle inferred from tri-axial deformation experiments on dry olivine crystals, Physics of the Earth and Planetary Interiors, 220, 37–49, 2013.

Drury, M. R.: Dynamic recrystallization and strain softening of olivine aggregates in the laboratory and the lithosphere, Geological Society, London, Special Publications, 243, 143–158, 2005.

Garel, F., Goes, S., Davies, D. R., Davies, J. H., Kramer, S. C., and Wilson, C. R.: Interaction of subducted slabs with the mantle transition-zone: A regime diagram from 2-D thermo-mechanical models with a mobile trench and an overriding plate, Geochem. Geophys. Geosyst., 15, 1739–1765, https://doi.org/10.1002/2014GC005257, http://dx.doi.org/10.1002/2014GC005257, doi:10.1002/2014GC005257, 2014.

Goetze, C. and Evans, B.: Stress and temperature in the bending lithosphere as constrained by experimental rock mechanics, Geophys. J. Int., 59, https://doi.org/10.1111/j.1365-246X.1979.tb02567.x, https://doi.org/10.1111/j.1365-246X.1979.tb02567.x, 1979.

Montési, L. G. and Hirth, G.: Grain size evolution and the rheology of ductile shear zones: from laboratory experiments to postseismic creep, Earth and Planetary Science Letters, 211, 97 – 110, https://doi.org/https://doi.org/10.1016/S0012-821X(03)00196-1, http://www.sciencedirect.com/science/article/pii/S0012821X03001961, 2003.

Turcotte, D. and Schubert, G. (1982). *Geodynamics: Applications of continuum physics to geological problems*. Cambridge University Press, New York, second edition.